JOC Articles

Synthesis and Structural and Photoswitchable Properties of Novel Chiral Host Molecules: Axis Chiral 2,2′-Dihydroxy-1,1′-binaphthyl-Appended *stiff*-Stilbene[1]

Toshiaki Shimasaki,[†,‡] Shin-ichiro Kato,[†,‡] Keiko Ideta,[§] Kenta Goto,[†] and Teruo Shinmyozu*,[†]

Institute for Materials Chemistry and Engineering (IMCE) and Department of Molecular Chemistry, Graduate School of Sciences, Kyushu University, Hakozaki 6-10-1, Higashiku, Fukuoka 812-8581, and IMCE, 6-1 Kasuga-koh-en, Kasuga 816-8580, Japan

shinmyo@ms.ifoc.kyushu-u.ac.jp

Received June 1, 2006

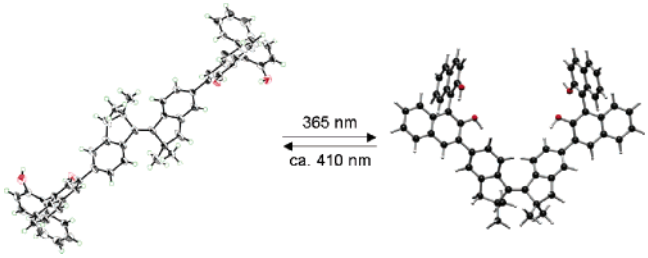

Novel photoswitchable chiral hosts having an axis chiral 2,2′-dihydroxy-1,1′-binaphthyl (BINOL)-appended *stiff*-stilbene, *trans*-(*R*,*R*)- and -(*S*,*S*)-**1**, were synthesized by palladium-catalyzed Suzuki−Miyaura coupling and low-valence titanium-catalyzed McMurry coupling as key steps, and they were fully characterized by various NMR spectral techniques. The enantiomers of *trans*-**1** showed almost complete mirror images in the CD spectra, where two split Cotton effects (exciton coupling) were observed in the β-transitions of the naphthyl chromophore at 222 and 235 nm, but no Cotton effect was observed in the *stiff*-stilbene chromophore at 365 nm. The structures of (*R*)-**10** and *trans*-(*R*,*R*)-**1** were confirmed by X-ray structural analysis. The optimized structure of *cis*-**1** by MO calculations has a wide chiral cavity of 7−8 Å in diameter, whereas *trans*-**1** cannot form an intramolecular cavity based on the X-ray data. Irradiation of (*R*,*R*)-*trans*-**1** with black light (λ = 365 nm) in CH_3CN or benzene at 23 °C led to the conversion to the corresponding *cis*-isomer, as was monitored by ^{1}H NMR, UV−vis, and CD spectra. At the photostationary state, the *cis*-**1**/*trans*-**1** ratio was 86/14 in benzene or 75/25 in CH_3CN. On the other hand, irradiation of the *cis*-**1**/*trans*-**1** (75/25) mixture in CH_3CN with an ultra-high-pressure Hg lamp at 23 °C (λ = 410 nm) led to the photostationary state, where the *cis*-**1**/*trans*-**1** ratio was estimated to be 9/91 on the basis of the ^{1}H NMR spectra. The *cis*−*trans* and *trans*−*cis* interconversions could be repeated 10 times without decomposition of the C═C double bond. Thus, a new type of photoswitchable molecule has been developed, and *trans*-**1** and *cis*-**1** were quite durable under irradiation conditions. The guest binding properties of the BINOL moieties of *trans*- and *cis*-(*R*,*R*)-**1** with F^-, Cl^-, and $H_2PO_4^-$ were examined by ^{1}H NMR titration in $CDCl_3$. Similar interaction with F^- and Cl^- was observed in *trans*-**1** (host/guest = 1/1, $K_{assoc} = (1.0 \pm 0.13) \times 10^3$ for F^- and $(4.6 \pm 0.72) \times 10^2$ M^{-1} for Cl^-) and *cis*-**1** (host/guest = 1/1, $K_{assoc} = (1.0 \pm 0.13) \times 10^3$ for F^- and $(5.9 \pm 0.69) \times 10$ M^{-1} for Cl^-), but $H_2PO_4^-$ interacted differently: the *cis*-isomer formed the 1/1 complex ($K_{assoc} = (9.38 \pm 2.67) \times 10$ M^{-1}), whereas multistep equilibrium was expected for the *trans*-isomer.

Introduction

In recent years, artificial molecules based on photoisomerization of double bonds have been developed as molecular motors,[2] switches,[3] machines,[4] etc.[5] As the pioneering study of molecular machines using this photoisomerization process, Shinkai et al. employed the azobenzene core attached to a bis(crown ether) framework as a metal cation recognition site. In the *cis*-form of the azobenzene moiety, the bis(crown ether) binds a Rb cation, whereas the Rb cation is released in the *trans*-form, and this *cis*−*trans* switching system of the azobenzene core was used as a membrane transporter.[4a,b] Since then, the

* To whom correspondence should be addressed. Phone: +81 92 642 2716. Fax: +81 92 642 2735.
† IMCE, Kyushu University.
‡ Department of Molecular Chemistry, Kyushu University.
§ IMCE, Kasuga.

10.1021/jo061127v CCC: $37.00
Published on Web 01/13/2007

azobenzene photoisomerization process has been widely used for the construction of various functional systems such as interlocked molecules, a scissor-like molecule, molecular hinges, etc.[4] Stilbenes have been an alternative class of compounds for the *cis*−*trans* photochemical switching system. On the other hand, reports on artificial functional molecules using the photoisomerization of C═C double bonds have appeared,[3,4c] but the *cis*-isomer of stilbene has absorption bands in the short-wavelength region relative to those of the *trans*-isomer. Therefore, selective irradiation of the *cis*- and *trans*-isomers is rather difficult, and UV light irradiation of the unstable *cis*-isomer results in partial decomposition via photolysis. Recently, Feringa et al.[2a,c] and Harada et al.[2a,c] have developed quite interesting molecular motors,[1] where one directional rotation of the overcrowded C═C bond occurs with high efficiency, and the overcrowded C═C bond causes its absorption band to shift to the longer wavelength region. New photoswitching systems using the photoisomerization of a tetraethynylethene having an absorption band in the longer wavelength region relative to that of the unsubstituted stilbene have been developed by Diederich et al.[4] Both the *trans*- and *cis*-stilbenes show strong UV absorption bands, and the bands at the longer wavelengths extend to ca. 300 nm in hexane at room temperature in both isomers, but the intensity of the band is lower in the *cis*-isomer than in the *trans*-isomer,[5] whereas the bands at the longer wavelength of the *cis*- and *trans*-azobenzenes appear in the visible region. This makes azobenzenes more attractive as a *cis*−*trans* photoswitching system. We have been interested in *stiff*-stilbenes, in which the rotation around the vinyl−phenyl bond is blocked by alicyclic bonds, because their longer wavelength absorption bands appear in the visible region. *stiff*-Stilbene was first reported by Majerus et al.,[7] and its structural and electrochemical properties,[8] excited-state behaviors,[9] and isomerization pathway have been reported,[10] in comparison with the corresponding properties of the stilbenes. The photochemical isomerization of stilbenes is understood to proceed via the "hula-twist" (HT) process, whereas that of the *stiff*-stilbenes is reported to proceed via a "one-bond flipping" process because the phenyl ring constraints do not allow any type of HT process.[10b] *stiff*-Stilbene is considered to be a better *cis*−*trans* switching system compared to the stilbenes because visible light can be used for the *cis*−*trans* photochemical isomerization and selective irradiation of the absorption band due to the C═C double bond of the *cis*-isomer becomes much easier. In spite of these advantages, *stiff*-stilbene has not yet been applied to the photochemical *cis*−*trans* switching system so far. If the isomerization efficiency and the location of the absorption bands of the stilbenes are comparable to those of the azobenzenes, stilbenes should be more useful for the development of new photoswitchable artificial host molecules due to their higher thermal stability.

SCHEME 1. Idea for a Novel Photoswitchable Chiral Host System, *trans*-1 and *cis*-1

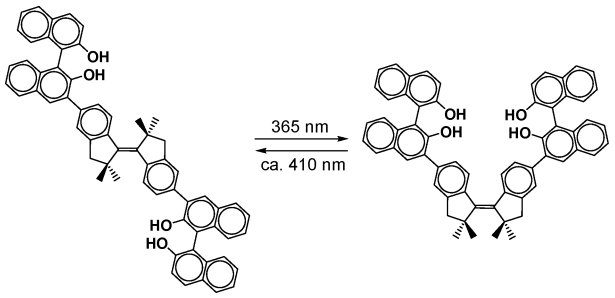

We designed *stiff*-stilbene with four methyl groups around the olefin because the introduction should lower the energy barrier for photoisomerization.[11] In addition, we designed a way to introduce chirality to the *stiff*-stilbene core because many photoswitchable artificial molecules using the isomerization of the double bond have been developed as already described, but only a few photoswitchable artificial molecules having a chirality for chiral recognition have been reported[4f] except in the field of biochemistry and polymer chemistry, to the best of our knowledge. Therefore, we considered that the development of new photoswitchable chiral hosts should be very useful for the chiral recognition of organic guests and their release after photochemical conversion (Scheme 1). Such systems may be newly categorized as a type of molecular machine, and the system may be applicable as a novel chiral molecular transporter, a light-driven reaction field, and a drug delivery system. As a

(1) Photoswitchable Host Molecules. 1.

(2) For reviews on molecular motors using the isomerization of double bonds, see: (a) Feringa, B. L. *Molecular Switches*; Wiley-VCH: New York, 2003; Chapter 5. (b) Journey, A.; Credi, A.; Venturi, M. *Molecular Devices and Machines*; Wiley-VCH: New York, 2004; Chapter 13. (c) Feringa, B. L. *Acc. Chem. Res.* **2001**, *34*, 504−513.(d) Schalley, C. A.; Beizai, K.; Vögtle, F. *Acc. Chem. Res.* **2001**, *34*, 465−476. (e) Kottas, G. S.; Clarke, L. L.; Horinek, D.; Michl, J. *Chem. Rev.* **2005**, *105*, 1281−1376. (f) Kinbara, K.; Aida, T. *Chem. Rev.* **2005**, *105*, 1377−1400.

(3) For reviews on molecular switches using the isomerization of double bonds, see: (a) Journey, A.; Credi, A.; Venturi, M. *Molecular Devices and Machines*; Wiley-VCH: New York, 2004; Chapters 4 and 7. (b) Irie, M.; Kato, M. *J. Am. Chem. Soc.* **1985**, *107*, 1024−1028.

(4) For reviews on molecular machines using the isomerization of double bonds, see: (a) Feringa, B. L. *Molecular Switches*; Wiley-VCH: New York, 2003; Chapters 7 and 9. (b) Journey, A.; Credi, A.; Venturi, M. *Molecular Devices and Machines*; Wiley-VCH: New York, 2004; Chapters 8, 12, and 13. (c) Balzani, V.; Credi, A.; Raymo, F. M.; Stoddart, J. F. *Angew. Chem., Int. Ed.* **2000**, *39*, 3348−3391. (d) Harada, A. *Acc. Chem. Res.* **2001**, *34*, 456−464. (e) Ballardini, D.; Balzani, V.; Credi, A.; Gandolfi, M. T.; Venturi, M. *Acc. Chem. Res.* **2001**, *34*, 445−455. Molecular machines using the isomerization of double bonds: (f) Murakami, H.; Kawabuchi, A.; Matsumoto, R.; Ito, T.; Nakashima, N. *J. Am. Chem. Soc.* **2005**, *127*, 15891−15899. (g) Muraoka, T.; Kinbara, K.; Aida, T. *Nature* **2006**, *440*, 512−515. (h) Nagamani, S. A.; Norikane, Y.; Tamaoki, N. *J. Org. Chem.* **2005**, *70*, 9304−9313. (i) Rojanathanes, R.; Pipoosananakaton, B.; Tuntulani, T.; Bhanthumnavin, W.; Orton, J. B.; Cole, S. J.; Hursthouse, M. B.; Grossel, M. C.; Sukwattanasinitt, M. *Tetrahedron* **2005**, *61*, 1317−1324 and references therein.

(5) Gobbi, L.; Seiler, P.; Diederich, F. *Helv. Chim. Acta* **2000**, *83*, 1711−1723.

(6) Calvin, C.; Alter, W. *J. Chem. Phys.* **1951**, *19*, 765−767.

(7) Majerus, G.; Yax, E.; Ourisson, G. *Bull. Soc. Chem. Fr.* **1967**, *11*, 4143−4147.

(8) For an example of the geometry of *stiff*-stilbene, see: (a) Schaefer, W. P. *Acta Crystallogr., Sect. C* **1995**, *C51*, 2364−2366. (c) Spiteller, P.; Jovanovic, J.; Spiteller, M. J. *Magn. Reson. Chem.* **2003**, *41*, 475−477. (d) Shimasaki, T.; Kato, S.; Shinmyozu, T. Unpublished result. (e) Ogawa, K.; Harada, J.; Tomoda. S. *Acta Crystallogr.* **1995**, *B51*, 240−248. For an example of the photophysics of a *stiff*-stilbene analogue, see: (f) Ogawa, K.; Suzuki, H.; Futakami, M. *J. Chem. Soc., Perkin trans. 2* **1988**, 39−43. (g) Rettig, W.; Majenz, W.; Herter, R.; Létard, J-F.; Lapouyade, R. *Pure. Appl. Chem.* **1993**, *65*, 1699−1704. (h) Vogel, J.; Schneider, S.; Dörr, F. *Chem. Phys.* **1984**, *90*, 387−398.

(9) (a) Hohlneicher, G.; Wrzal, R.; Lenoir, D.; Frank, R. *J. Phys. Chem A* **1999**, *103*, 8969−8975. (b) Improta, R.; Santoro, F.; Dietl, C.; Papastathopoulos, E.; Gerber, G. *Chem. Phys. Lett.* **2004**, *387*, 509−516. (c) Improta, R.; Santoro, F. *J. Phys. Chem. A* **2005**, *109*, 10058−10067.

(10) (a) Waldeck, D. H. *Chem. Rev.* **1991**, *91*, 415−436. (b) Liu, R. S. H. *Acc. Chem. Res.* **2001**, *34*, 555−562. (c) Saltiel, J.; Mace, J. E.; Watkins, L. P.; Gormin, D. A.; Clark. R. J.; Dmitrenko, O. *J. Am. Chem. Soc.* **2003**, *125*, 16158−16159. (d) Fuss, Werner, Kosmidis, C.; Schmid, W. E.; Trushin, S. A. *Angew. Chem., Int. Ed.* **2004**, *43*, 4178−4182.

(11) Newman, M. S. *Steric Effects in Organic Chemistry*; John Wiley & Sons: New York, 1956; Chapter 11.

chiral recognition agent, we chose 2,2′-dihydroxy-1,1′-binaphthyl (BINOL), which has been proven to have the exquisite ability as an optical resolution agent for amino acids,[12a,b,d] sulfoxides,[12f] amino alcohols,[12h] sugar acids,[12i] and so on[12c,g] in the solid state and in solution.[12a,b,i] Moreover, the chiral cavity formed by several BINOL units showed good complexation ability for various sugar molecules.[12j] In this context, our combined interests in the photochemical isomerization of the *stiff*-stilbenes and chiral recognition using the axis chiral BINOL moiety led us to the design and synthesis of the first generation of a reversibly photoswitchable chiral molecule, **1**, with a *stiff*-stilbene core linked to two enantiomerically pure BINOL moieties. In *cis*-**1**, a chiral intramolecular cavity can be formed by two BINOL moieties, whereas no such intramolecular cavity can be formed in *trans*-**1**. As a final objective, we planned to develop novel chiral photoswitchable host molecules which should satisfy the following requirements: (1) a highly efficient *cis*−*trans* photochemical isomerization of C═C double bonds and (2) chiral recognition and inclusion in the *cis*-form and release of the chiral guests in the *trans*-form upon irradiation.

We now report the synthesis of the first-generation host molecules and their characterization based on various NMR, UV−vis, and circular dichroism (CD) spectra, as well as X-ray structural analysis and theoretical calculations using the B3LYP/6-31G* theory. The isomerization from *trans*-(*R*,*R*)-**1** to *cis*-(*R*,*R*)-**1** and vice versa in solution will be demonstrated by photoirradiation with 365 nm light (*trans* to *cis*) and ca. 410 nm light (*cis* to *trans*), respectively. This was the first example where the reversible *cis*−*trans* photoisomerization of *stiff*-stilbenes was used to build a photoswitchable host.

Results and Discussion

Synthesis. The synthesis of 5-bromo-2,2-dimethylindanone (**6**) has already been accomplished by the carbopalladation of nitriles,[13] but we synthesized it using an alternative route (Scheme 2). 3-Bromotoluene (**2**) was converted into 1-bromo-3-benzyl bromide (**3**) with NBS in the presence of AIBN in benzene.[14] The resulting bromide was transformed into the methyl ester **4** by the nucleophilic addition of the lithiated methyl 2-methylpropanoate, which was prepared from the methyl 2-methylpropanoate and LDA.[1n] The carboxylic acid **5** was obtained as colorless crystals by alkaline hydrolysis of the methyl ester **4**. The intramolecular Friedel−Crafts cyclization of the acid chloride of **5** afforded **6** (82%).

During the initial stage of this study, we attempted to synthesize the C═C double bond by the homocoupling of **6** with the low-valent Ti prepared from $TiCl_4$ and 2 mol equiv of Zn powder, but the desired 2,2,2′,2′-tetramethyl-5,5′-dibromo-1,1′-indanylindane could not be obtained by this method. Therefore, we modified the synthetic route to the first introduction of the substituent to the benzene ring, followed by formation of the C═C double bond. As the substituent of the indanone moiety, we first chose 2,2′-dihydroxy-1,1′-binaphthyl (BINOL, **7**). The MOM-protected BINOLs (*R*)-**8** and (*S*)-**8** were readily prepared from the commercially available (*R*)- or (*S*)-BINOL **7** in almost quantitative yields, respectively.[15b] (*R*)-**8** was treated with 1.1 equiv of *n*-BuLi (hexane solution) in THF at −78 °C for 4 h. $B(OMe)_3$ (1.2 equiv) was then added to the mixture and the resulting mixture stirred at room temperature for 12 h to give 3-(dimethoxyboryl)-BINOL-MOM [(*R*)-**9**] as a colorless oil. We observed the cleavage of the methoxymethyl group located at the ortho position to the $B(OMe)_2$ group when the solvent was completely removed, probably due to the Lewis acidity of the boronic acid ester. Therefore, we used (*R*)-**9** in the next reaction without further purification. The crude (*R*)-**9** and the 5-bromoindanone **6** were coupled under the $Pd(PPh_3)_4$-catalyzed Suzuki−Miyaura reaction conditions to afford the (*R*)-3-(dimethoxyboryl)-BINOL-MOM-indanone (*R*)-**10** (67%).[15] On the basis of similar synthetic procedures, (*S*)-**10** was also prepared from (*S*)-**8** (57%). The Suzuki−Miyaura coupling reaction of the compounds, in which one or two MOM groups were deprotected, was unsuccessful, probably because of the formation of a metal complex between the hydroxyl group of the BINOL and palladium.

The McMurry coupling of (*R*)-**10** using low-valent Ti,[16] followed by deprotection of the MOM groups with dilute aq HCl in CH_2Cl_2/MeOH, provided a mixture of the *trans*- and

SCHEME 2. Synthesis of *trans*-(*R*,*R*)-1 and *trans*-(*S*,*S*)-1[a]

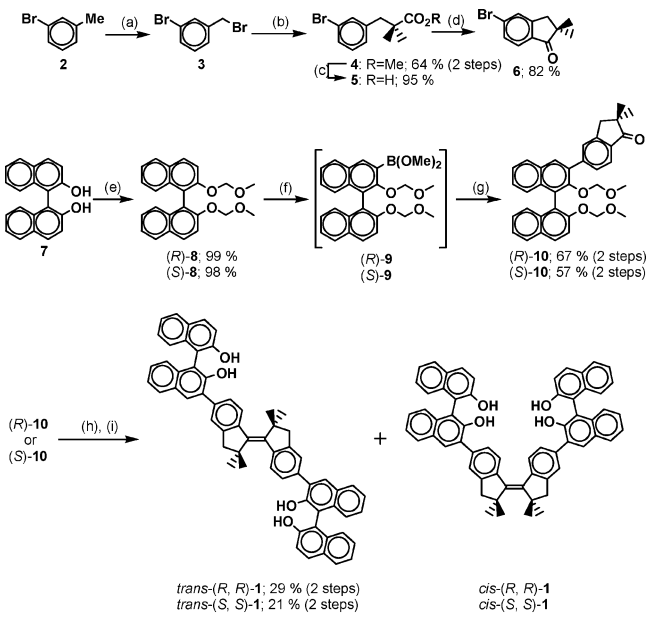

[a] Reagents and conditions: (a) NBS (1.1 mol equiv), AIBN, benzene, reflux; (b) LDA (1.3 mol equiv), methyl 2-methylpropanoate (1.0 mol equiv), THF, −78 °C to rt; (c) KOH (10 mol equiv), MeOH, H_2O, reflux; (d) $AlCl_3$ (1.0 mol equiv), CH_2Cl_2; (e) NaH (8 mol equiv), CH_3OCH_2Cl (2.0 mol equiv), THF, rt, 12 h; (f) *n*-BuLi (1.3 mol equiv), $B(OMe)_3$, THF, −78 °C to rt for 12 h; (g) compound **6**, toluene, satd aq Na_2CO_3, $Pd(PPh_3)_4$ (5 mol %), reflux; (h) $TiCl_4$ (3 mol equiv), Zn (6 mol equiv), THF, reflux; (i) 6 N aq HCl (3 drops), CH_2Cl_2/MeOH.

(12) (a) Zang, X. X.; Bradshaw, J. S.; Izatt, R. M. *Chem. Rev.* **1997**, *97*, 3313−3361. (b) Gokel, G. W.; Leevy, W. M.; Weber, M. E. *Chem. Rev.* **2004**, *104*, 2723−2750. (c) Imai, Y.; Tajima, N.; Sato, T.; Kuroda, R. *Chirality* **2002**, *14*, 604−609. (d) Lin, J.; Rajaram, A. R.; Pu, L. *Tetrahedron* **2004**, *60*, 11277−11281. (e) Kim, K. M.; Park, H.; Kim, H.-J.; Chin, J.; Nam, W. *Org. Lett.* **2005**, *7*, 3525−3527. (f) Liao, J.; Sun, X.; Cui, X.; Yu, K.; Zhu, Y. J.; Deng, J. *Chem.—Eur. J.* **2003**, *9*, 2611−2615. (g) Ouchi, A.; Zandomeneghi, G.; Zandomeneghi, M. *Chirality* **2002**, *14*, 1−11. (h) Pugh, V. J.; Hu, Q.-S.; Zuo, X.; Lewis, F. D.; Pu, L. J. Org. Chem. **2001**, *66*, 6136−6140. (i) Zhao, J.; Fyles, T. M.; James, T. D. *Angew. Chem., Int. Ed.* **2004**, *43*, 3461−3464. (j) Anderson, S.; Neidlein, U.; Gramlich, V.; Diederich, F. *Angew. Chem., Int. Ed.* **1995**, *34*, 1596−1600.

(13) Pletner, A. A.; Larock, R. C. *J. Org. Chem.* **2002**, *67*, 9428−9438.

(14) Shoesmith, J. B.; Slater, R. H. *J. Chem. Soc., Abstr.* **1926**, 214−223.

(15) (a) Bai, X.-L.; Liu, X.-D.; Wang, M.; Kang, C.-Q.; Gao, L.-X. *Synthesis* **2005**, *3*, 458−464. (b) Wu, T. R.; Shen, L.; Chong, J. M. *Org. Lett.* **2004**, *6*, 2701−2704. (c) Stock, H. T.; Kellogg, R. M. *J. Org. Chem.* **1996**, *61*, 3093−3105.

(16) (a) McMurry, J. E. *Chem. Rev.* **1989**, *89*, 1513−1524. (b) McMurry, J. E. *Acc. Chem. Res.* **1983**, *16*, 405−411.

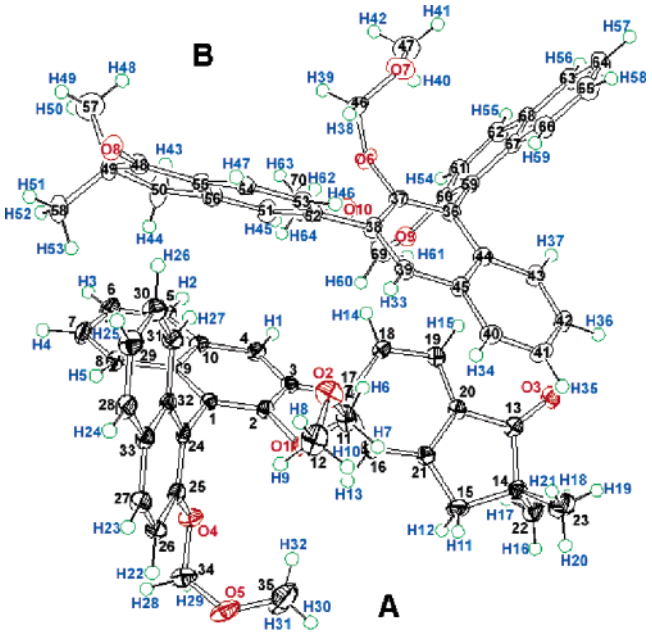

FIGURE 1. ORTEP drawing of (*R*)-**10**. Two crystallographically independent molecules (A and B) are observed in the unit cell. The atoms are drawn as 50% probability ellipsoids. Selected bond lengths (Å) and angles (deg) for molecule A: C1−C24, 1.504(5); C3−C17, 1.495(5); C13−O3, 1.218(4); C2−C1−C24−C25, 69.5(4); C2−C3−C17−C18, 129.9(4); C2−O1−C11−O2, 84.4(4); O4−C34−O5−C35, 63.8(4); C25−O4−C34−O5, 71.4 (4). Selected bond lengths (Å) and angles (deg) for molecule B: C36−C59, 1.498(5); C38−C52, 1.498(5); C48−O8, 1.219(4); C60−C59−C36−C37, 68.7(5); C37−C38−C52−C53, 129.5(4); C37−O6−C46−O7, 84.5(4); O1−C11−O2−C12, 68.7(4); O6−C46−O7−C47, 69.3(4); C60−O9−C69−O10, 71.5(4); O9−C69−O10−C70, 63.3(4).

cis-(*R*,*R*)-**1** in approximately a 5:1 ratio on the basis of the ^{1}H NMR spectrum. Similarly, *trans*-(*S*,*S*)-**1** was also obtained (21%) using procedures similar to those described for *trans*-(*R*,*R*)-**1** from (*R*)-**10**. Thus, the desired pure *trans*-(*R*,*R*)- and -(*S*,*S*)-**1** were obtained in eight steps in a 6−10% overall yield (Scheme 2). The *trans*-isomers were purified by silica gel column chromatography followed by precipitation from CH_2Cl_2/hexane. However, isolation of the pure *cis*-isomer from the *cis*/*trans* (1/5) mixture was quite difficult because of the rapid photochemical isomerization of the *cis*-isomer to the *trans*-isomer during the chromatographic separation.

Structural Properties. The structure of the synthetic intermediate (*R*)-**10** was confirmed by an X-ray crystallographic analysis (Figure 1). The space group of the crystal is $P2_1$, and the two crystallographically independent molecules are located in the unit cell. Both molecules A and B adopted the C_1 symmetry, but the bond lengths, angles, and torsions were slightly different from each other.

The A and B molecules form a continuous dimeric structure via intermolecular multipoint interactions such as CH−π and CH−O.[17] The distances between C4 (naphthyl) and H38 (MOM methylene) as well as C19 (indanyl) and H58 (naphthyl) are 2.90 and 2.79 Å, respectively. These short contacts may be ascribed to the CH−π interactions. Similar CH−π-type interactions are expected between C6 (naphthyl) and H44 (indanyl methylene) (distance 2.85 Å), C8 (naphthyl) and H47 (indanyl phenyl) (2.79 Å), C43 (naphthyl) and H15 (indanyl phenyl) (2.78 Å), and C44 (naphthyl) and H15 (indanyl phenyl) (2.85 Å). The unit cells are connected via a CH−O interaction between the two kinds of peri-protons of the naphthyl moiety and the carbonyl group of the indanone moiety to form columnar structures along the *a* axis (Figure 2). Each column is linked via CH−O interactions between a hydrogen atom of the methyl group of the indanone moiety and an oxygen of the methoxy group in the binaphthyl moiety (O3−H23, 2.40 Å; O3−H24, 2.56 Å; O4−H46, 2.55 Å; O4−H47, 2.65 Å; O8−H55, 2.42 Å; O8−H56, 2.56 Å; O9−H14, 2.56 Å; O9−H15, 2.66 Å; O10−H21, 2.68 Å). The torsion angles between the naphthyls (C2−C1−C24−C25) and naphthyl and indanone (C2−C3−C17−C18) of molecule A are 69.5° (B, 68.7°) and 51.0° (50.7°), respectively.

We also examined the X-ray analysis of *trans*-(*R*,*R*)-**1** recrystallized from dimethoxyethane (DME) and confirmed the DME clathrate of *trans*-(*R*,*R*)-**1** (Figure 3), and the structural parameters were compared with calculated ones at the B3LYP/6-31G* level of theory (Table 1). The space group is monoclinic $P2_1$, similar to the space group of (*R*)-**10**. The central C═C double bond length (C1−C32) is 1.349 Å, and this is comparable to that of *trans*-2,2,2′,2′-tetramethyl-*stiff*-stilbene (1.357 Å).[8d] The torsion angle of 164.2° (C8−C1−C32−C39) indicates that the double bond is skewed by 15.8° from planarity due to the

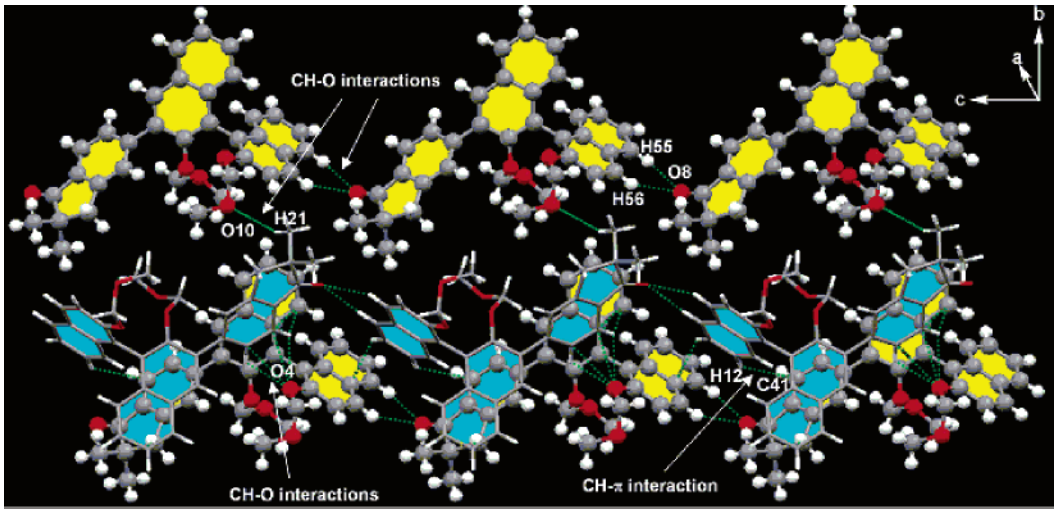

FIGURE 2. Packing diagram of (*R*)-**10**. Molecules of A and B are shown by capped sticks and balls and sticks, respectively. Dashed lines are within the sum of the van der Waals radius.

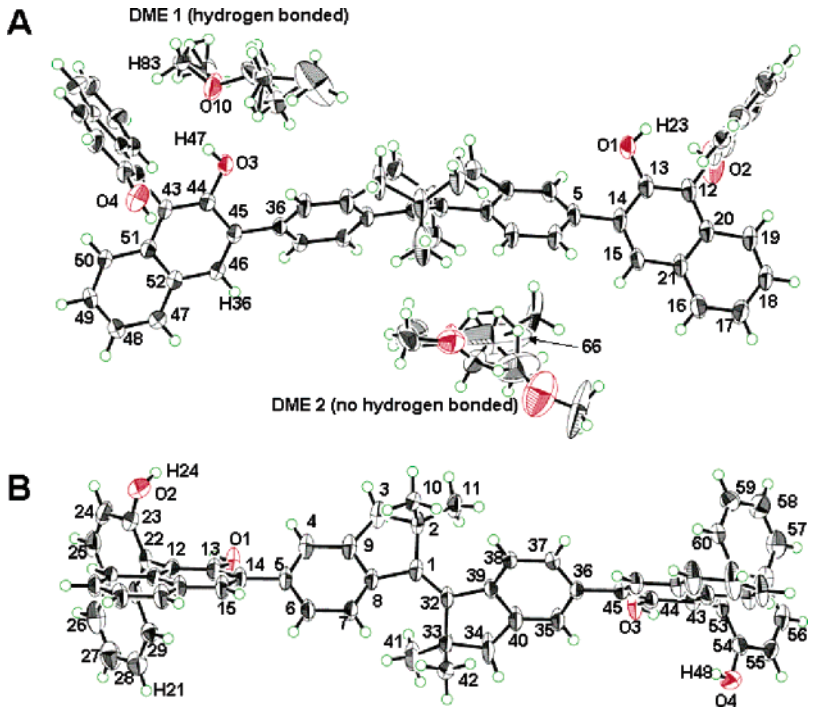

FIGURE 3. ORTEP drawing of *trans*-(*R*,*R*)-**1**: (A) atoms drawn as 50% probability ellipsoids; (B) skeleton of *trans*-(*R*,*R*)-**1**. DME molecules were omitted for clarity. Selected bond lengths (Å) and angles (deg): C1−C32, 1.349(5); C5−C14, 1.503(5); C12−C22, 1.481(6); C36−C45, 1.483(5); C43−C53, 1.494(5); H47−O10, 2.112; C4−C5−C14−C13, 48.4(6); C8−C1−C32−C39, −164.2(4); C13−C12−C22−C23, −97.9(5); C35−C36−C45−C44, 41.1(5); C44−C43−C53−C54, 102.0(4).

TABLE 1. X-ray and Calculated Structural Data of *cis*- and *trans-stiff*-Stilbene

	bond lengths (Å)		torsion angles (deg)	
	C1−C32	C8−C1−C32−C39	C13−C12−C22−C23	C4−C5−C13−C14
trans-(*R*,*R*)-**1** (X-ray)	1.349(5)	164.2(4)	−97.9 (102.0)[c]	48.4 (41.1)[d]
trans-(*R*,*R*)-**1** (calcd)[a]	1.366[b]	164.1	−92.6 (84.2)[c]	49.0 (41.8)[d]
cis-(*R*,*R*)-**1** (calcd)[a]	1.375[b]	28.8	−91.0 (80.6)[c]	48.6 (48.5)[d]

[a] The structures of *trans*- and *cis*-(*R*,*R*)-**1** were optimized at the B3LYP/6-31G* level of theory. [b] The C═C double bond of the calculated structure is C1−C1′. [c] Torsion angle of another naphthyl−naphthyl moiety. [d] Torsion angle of another BINOL−*stiff*-stilbene moiety.

steric congestion around the double bond. The torsion angles between *stiff*-stilbene and BINOL (C4−C5−C14−C13 and C35−C36−C45−C44) and the naphthyl groups (C13−C12−C22−C23 and C44−C43−C53−C54) are 48.4°, 41.1°, −97.9°, and 102.0°, respectively. The two BINOL groups were widely separated (O1−O3, 13.216 Å; O2−O4, 20.299 Å; O1−O4, 16.761 Å; O2−O3, 16.620 Å), similarly to those of the calculated structure (O1−O3, 13.525 Å; O2−O4, 18.929 Å; O1−O4, 16.207 Å; O2−O3, 16.607 Å).

The packing diagram of *trans*-(*R*,*R*)-**1** with DME is shown in Figure 4. Two kinds of DME molecules are shown as space-filling models: the DME with atom colors formed hydrogen bonds with the BINOL hydroxyl group, while no hydrogen bonding was observed in the DME with yellow color. The non-hydrogen-bonded DME molecules showed severe disorder due to thermal rotation centering around one of methylenes (C66) in the crystal. The distance of the hydrogen bond between H47 (BINOL O1) and O10 (DME) is 2.112 Å. Moreover, CH−π interactions are expected between the naphthyl ring of *trans*-(*R*,*R*)-**1** (C56, C60, C61, and C62) and the methyl hydrogen H83 of DME (distance 2.79, 2.90, 2.83, and 2.47 Å, respectively). Similar CH−π interactions are also observed between C21 (naphthyl) and H28 (indanyl) (2.84 Å), C24 and C25 (naphthyl) and H36 (naphthyl) (2.81 and 2.90 Å), C35 (indanyl) and H21 (naphthyl) (2.87 Å), and C51 and C52 (naphthyl) and H4 (indanyl) (2.90 and 2.77 Å). In addition, a OH−π-type interaction is also expected between C47 (naphthyl) and H23 (naphthyl hydroxyl) (2.79 Å).

The B3LYP/6-31G*-optimized structure of *cis*-(*R*,*R*)-**1** is shown in Figure 5. *trans*-(*R*,*R*)-**1** was estimated to be more stable than *cis*-(*R*,*R*)-**1** by 9.12 kcal/mol. The four hydroxyl groups are directed toward the inside of the molecule. The dihedral angles of naphthyl−naphthyl (C23−C22−C12−C13), naphthyl−indanyl (C13−C14−C5−C6), and indanyl−indanyl (C8−C1−C1′−C8′) are predicted to be 91.1°, 51.4°, and 28.8°, respectively. The distances of C1−C1′, O1−O1′, O2−O2′, O1−O2′, and O2−O1′ are expected to be 1.376, 6.872, 9.854, 8.505, and 8.274 Å, respectively, and the size of the chiral cavity formed by the four BINOL OH groups is ca. 7−8 Å. In this cavity, various organic molecules may be included, and interesting inclusion phenomena due to the hydrogen bonds and $\pi-\pi$ and CH−π interactions may be observed in *cis*-(*R*,*R*)-**1**. In contrast, an intramolecular cavity is not expected for the *trans*-isomer. Moreover, the thermal stability of *cis*-(*R*,*R*)-**1** was

(17) (a) Bondi, A. *Phys. Chem.* **1964**, *68*, 441−451. (b) Tuduki, S.; Honda, K.; Uchimaru, T.; Mikami, M.; Tanabe, K. *J. Am. Chem. Soc.* **2000**, *122*, 3746−3753. (c) Shibasaki, K.; Fujii, A.; Mikami, N.; Tuduki, S. *J. Phys. Chem. A* **2006**, *110*, 4397−4404.

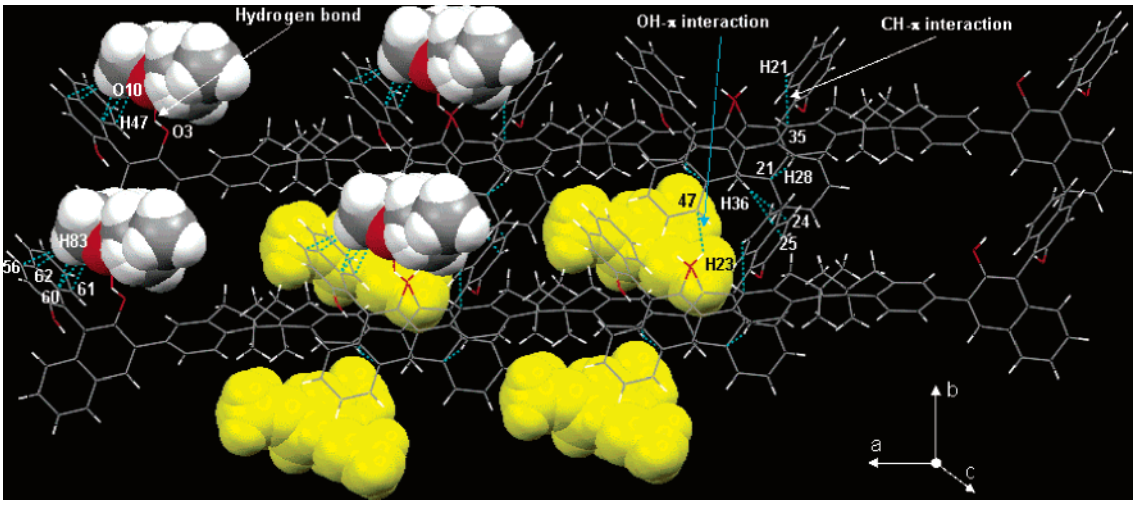

FIGURE 4. Packing diagram of *trans*-(*R*,*R*)-**1**. Two kinds of DME molecules are shown as space-filling models with atom colors (hydrogen bonds with BINOL-OH) and yellow (no hydrogen bond). Dashed lines are within the sum of the van der Waals radius.

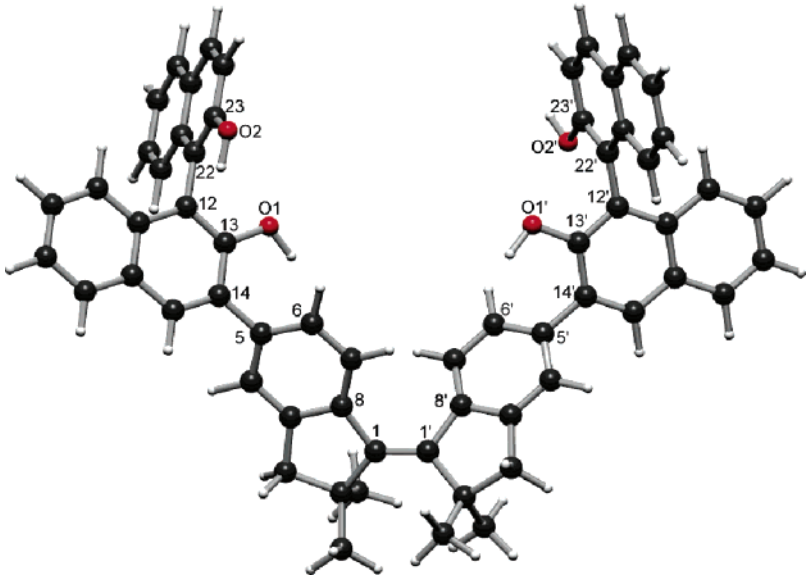

FIGURE 5. Optimized structure of *cis*-(*R*,*R*)-**1** using the B3LYP/6-31G* level of theory. Selected bond lengths (Å) and angles (deg): C1−C1′, 1.376; O1−O1′, 6.872; O2−O2′, 9.854; O1−O2′, 8.505; O1′−O2, 8.274; naphthyl−naphthyl (C23−C22−C12−C13 and opposite BINOL dihedral), naphthyl−indanyl (C13−C14−C5−C6 and opposite naphthyl−indanyl dihedral), indanyl−indanyl (C8−C1−C1′−C8′) of the optimized structure possess 91.1°, 51.4°, and 28.8° angles, respectively.

checked in benzene and monitored by ^{1}H NMR spectra. Consequently, we observed that the almost no thermal isomerization from *cis*-(*R*,*R*)-**1** to *trans*-(*R*,*R*)-**1** was observed under benzene reflux conditions for 12 h and vise versa. As our prediction, the BINOL-appended *stiff*-stilbene host molecules possessed quite high thermal stabilities. The NMR and mass spectra of *trans*-(*R*,*R*)- and -(*S*,*S*)-**1** supported their structures. Various NMR data [^{1}H (Figures S7 and S9, "S" indicating Supporting Information), ^{13}C (Figures S8 and S10), ^{1}H−^{1}H COSY (Figures S11 and S12),[18] HMBC (Figure S13),[19] HMQC (Figure S14)[20]] and the complete assignments for *trans*-(*R*,*R*)-**1** in CH_3CN are summarized in Table S1. The ^{1}H and ^{13}C NMR spectral data suggested a C_2 symmetric structure. The *trans*-geometry of (*R*,*R*)-**1** was confirmed by the NOE (1D DPFGSE) spectrum[21] of *trans*-(*R*,*R*)-**1** in CD_3CN solution (Figures S17 and S18).

Chiroptical Properties. To obtain information on the relationship between the stereochemical and chiroptical properties of both enantiomers of *trans*-**1**, the UV−vis and CD spectra as well as specific rotations were measured in CH_3CN.

(18) For an example of the ^{1}H−^{1}H COSY measurement, see: Braun, S.; Kalinowski, H.-O.; Berger, S. *150 and More Basic NMR Experiments A Practical Course*, 2nd expanded ed.; Wiley-VCH: New York, 1998; Chapter 10, Experiment 10.3.

(19) For an example of the HMBC measurement, see: Braun, S.; Kalinowski, H.-O.; Berger, S. *150 and More Basic NMR Experiments A Practical Course*, 2nd expanded ed.; Wiley-VCH: New York, 1998; Chapter 12, Experiment 12.4.

(20) For and example of the HMQC measurement, see: Braun, S.; Kalinowski, H.-O.; Berger, S. *150 and More Basic NMR Experiments A Practical Course*, 2nd expanded ed.; Wiley-VCH: New York, 1998; Chapter 12, Experiment 12.3.

(21) For an example of the DPFGSE (double pulsed field gradient spin echo) method−NOE, see: Braun, S.; Kalinowski, H.-O.; Berger, S. *150 and More Basic NMR Experiments A Practical Course*, 2nd expanded ed.; Wiley-VCH: New York, 1998; Chapter 11, Experiment 11.10.

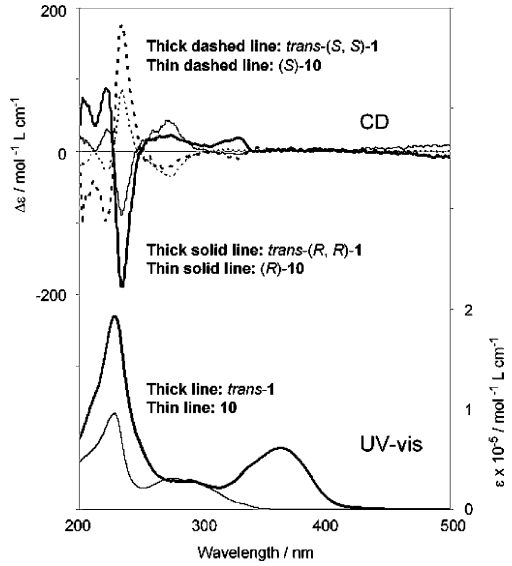

FIGURE 6. UV−vis spectra (lower) and CD spectra (upper) of both enantiomers of **10** and *trans*-**1** in CH_3CN: *trans*-(*R*,*R*)-**1** (thick solid line), *trans*-(*S*,*S*)-**1** (thick dashed line), (*R*)-**10** (thin solid line), (*S*)-**10** (thin dashed line).

We confirmed that the CD spectra of both enantiomers of the BINOL-MOM-indanone **10** as well as the chiral host **1** showed almost complete mirror images (Figure 6). The values of the specific rotation also supported the relationship of the enantiomers [$[\alpha]^{24}_D$ +168.3° (c = 1.00, CH_3CN) for (*R*)-**10**, +205.4° (c = 0.55, CH_3CN) for *trans*-(*R*,*R*)-**1**, −166.9° (c = 1.01, CH_3CN) for (*S*)-**10**, and −205.6° (c = 1.00, CH_3CN) for *trans*-(*S*,*S*)-**1**, respectively]. BINOL has an absorption band at ca. 225 nm (ϵ ca. 10000) due to the β-transitions (^1B_b) polarized along the long axis of the naphthyl chromophore,[22] whereas *trans*-2,2,2′,2′-tetramethyl-*stiff*-stilbene has an absorption band at around 326 nm (ϵ 20500).[9e] (*R*)-**10** showed almost the same absorption spectrum as the unsubstituted BINOL except the band at ca. 275 nm due to the naphthyl p-band (^1L_a, ϵ 3090). The longest wavelength absorption band (λ_{max}) of *trans*-(*R*,*R*)-**1** appeared at 362 nm (ϵ 61500) with no vibrational fine structures, and this is attributed to the *stiff*-stilbene with extended π-conjugation. This band is ascribed to the HOMO−LUMO transition, and the B3LYP/6-31G* level calculation predicted the band at 346 nm (Δ(HOMO−LUMO) = 82.7 kcal/mol). The intensity of the absorption band at 227 nm (ϵ 192000) due to the naphthyl β-transition of *trans*-(*R*,*R*)-**1** was 2-fold higher than that of (*R*)-**10**. In the CD spectrum of (+)-*trans*-(*R*,*R*)-**1**, relatively intense Cotton effects appeared at 235 nm ($\Delta\epsilon$ −190) and 222 nm ($\Delta\epsilon$ +88) probably due to the polarized β-transitions (^1B_b).[22]

It was reported that the counterclockwise minus helix (negative chirality) of the BINOL moieties induced the split Cotton effects, in which the longer wavelength extremum is negative and the shorter wavelength extremum is positive due to the exciton chirality (Figure 7).[23] In fact, (*R*)-BINOL was reported to show split Cotton effects, in which the first Cotton band is negative and the second one is positive at the β-band on the naphthyl moiety.[23] This was applicable to (−)-*trans*-(*S*,*S*)-**1** and should have the positive helix on the BINOL moieties. In **10**, very similar split Cotton effects due to the β-band of naphthyl chromophores were observed, but the intensities of the band and/or trough strengths were about half those of *trans*-**1** as shown by the thin line in Figure 5. The p-band (^1L_a, $\Delta\epsilon$(+20) ca. 270 nm) and α-band (^1L_b, $\Delta\epsilon$(+18) ca. 320 nm) may be ascribed to the polarization along the long and short axes of the naphthyl chromophore, respectively.

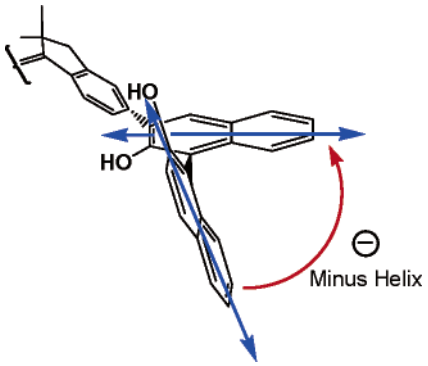

FIGURE 7. Two long axes of the naphthyl chromophores. (*R*)-**10** and *trans*-(*R*,*R*)-**1** constitute a counterclockwise helix.

Photochemical Isomerization between *trans*-(*R*,*R*)-1 and *cis*-(*R*,*R*)-1.[24]The photochemical isomerization process of **1** was examined. The deoxygenated benzene-d_6 solution of (+)-*trans*-(*R*,*R*)-**1** was irradiated with a black light (365 nm) in a Pyrex NMR tube at 23 °C, and the reaction was monitored by ^1H NMR spectra. The ratio of the *cis*- and *trans*-isomers was determined by the integral intensities of the benzylic proton signal of the *stiff*-stilbene moiety [*cis*, 3.45 ppm (J = 15.0 Hz) and 2.77 ppm (J = 15.0 Hz); *trans*, 2.99 ppm] (Figure 8). The amount of the *cis*-isomer gradually increased as the irradiation time increased, and the isomerization reached a photostationary state after 1 h of irradiation. The ratio of the *cis*- to *trans*-isomers was then estimated to be 86/14 on the basis of the ^1H NMR signals of the benzylic protons. A significant solvent effect was observed, and a ratio of 75/25 was obtained in a highly polar CD_3CN solution at the photostationary state.

The reverse photochemical isomerization from *cis*-(*R*,*R*)-**1** to *trans*-(*R*,*R*)-**1** was also monitored by ^1H NMR spectra (Figure 9). The deoxygenated CD_3CN solution of a mixture of *cis*-(*R*,*R*)-**1** and *trans*-(*R*,*R*)-**1** (75/25) was irradiated using an ultra-high-pressure Hg lamp (500 W) with a cutoff filter (λ = ca. 410 nm) in a Pyrex NMR tube at 23 °C. The reaction reached the photostationary state after a 10 min irradiation, where the *cis*/*trans* ratio was 9/91. This reaction also showed a significant solvent effect; the ratio of *cis* to *trans* was 23/77 at the photostationary state in benzene when the 86/14 mixture of *cis*- and *trans*-(*R*,*R*)-**1** was used.

(22) For an example of the assignment of transition bands in BINOL, see: (a) Hanazaki, I.; Akimoto, H. *J. Am. Chem. Soc.* **1972**, *94*, 4102−4106. (b) Mason, S. F.; Seal, R. H. *Tetrahedron* **1974**, *30*, 1671−1682.

(23) Berova, N.; Nakanishi, K.; Woody, R. W. *Circular Dichroism: Principle and Applications*, 2nd ed.; Wiley-VCH: New York, 2000; Chapter 12.

(24) We compared the rate of the *cis*−*trans* photochemical isomerization of *trans*-(*R*,*R*)-**1** with azobenzene upon irradiation with 365 and ca. 410 nm light at 23 °C in benzene, and the reactions were monitored by ^1H NMR spectra. The photoisomerization of *trans*-(*R*,*R*)-**1** to *cis*-(*R*,*R*)-**1** reached 86/14 (*cis*/*trans*) after 60 min of irradiation and was ca. 2.3 times faster than that of azobenzene (84/16 after 140 min of irradiation). On the other hand, the rate of photochemical isomerization from *cis*-(*R*,*R*)-**1** to *trans*-(*R*,*R*)-**1** (23/77 after 20 min) was almost similar to that of azobenzene (22/78 after 20 min) in benzene. Comparison of the rates of *trans* to *cis* photoisomerization between **1** and azobenzene in benzene and those of the reverse isomerization are summarized in Figures S23 and S24, respectively. For the rates of isomerization of azobenzene, see: Yamashita, S.; Ono, H.; Toyama, O. *Bull. Chem. Soc. Jpn.* **1962**, *35*, 1849−1853.

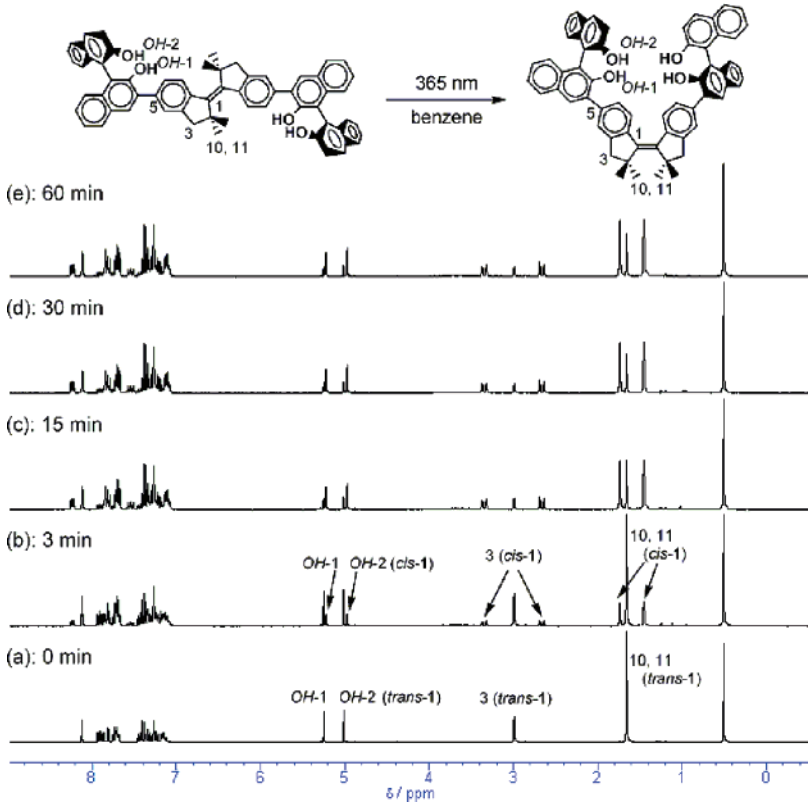

FIGURE 8. ^{1}H NMR spectra of the photoisomerization of *trans*-(*R*,*R*)-**1** to *cis*-(*R*,*R*)-**1** upon irradiation with 365 nm light in C_6D_6 at 23 °C: (a) 0 min, (b) 3 min, (c) 15 min, (d) 30 min, and (e) 60 min [photostationary state (*trans*-(*R*,*R*)-**1**/*cis*-(*R*,*R*)-**1** = 86/14)].

Thus, the *cis*−*trans* photochemical interconversion was conveniently monitored by ^{1}H NMR spectra, whereas the interconversion in very diluted solutions could be monitored by UV−vis and CD spectra. The photochemical isomerization process of *trans*-(*R*,*R*)-**1** to *cis*-(*R*,*R*)-**1** with 365 ± 5 nm light from a Xe lamp in the fluorescence photometer was also monitored by UV−vis and CD spectra in CH_3CN at 23 °C (Figure 10). The reaction reached the photostationary state after a 60 min irradiation. The gradual decrease in the intensity of the absorption band at 363 nm and corresponding gradual increase in the intensity of the band at ca. 410 nm due to the *stiff*-stilbene chromophore were observed through an isosbestic point at 391 nm. The intensity of the band at ca. 265 nm due to the *cis*-*stiff*-stilbene chromophore and naphthyl p-band also gradually increased through the isosbestic point at 252 and 313 nm. Although the α- and *β*-bands of the naphthyl chromophores showed almost no change in the CD spectra, the *cis*-*stiff*-stilbene chromophore or naphthyl p-band at ca. 265 nm slightly increased with an increase of the amount of the *cis*-isomer, but we could not explain the reason at present because several chromophores were overlapped in this region.

The reverse isomerization of *cis*-(*R*,*R*)-**1** to *trans*-(*R*,*R*)-**1** was also monitored by UV−vis and CD spectra in CH_3CN at 23 °C (Figure 11). The photostationary state obtained by the irradiation (60 min) of the CH_3CN solution of *trans*-(*R*,*R*)-**1** was irradiated with 410 ± 5 nm light, and the irradiation reached another photostationary state after 100 min. Both the naphthyl α-, *β*-, and p-bands and *stiff*-stilbene absorption bands were regenerated in the UV−vis spectra and CD spectrum of *trans*-(*R*,*R*)-**1** through the isosbestic points. A series of isosbestic points indicated clean interconversions between the *cis*- and *trans*-isomers. Thus, *trans*-**1**−*cis*-**1** represented a novel molecular photoswitch.

To check the stability of the *stiff*-stilbene core to the photochemical *cis*−*trans* interconversion, resistance against photofatigue experiments were carried out in deoxygenated CH_3CN solution and monitored by UV spectra. A solution of the enantiopure *trans*-(*R*,*R*)-**1** (1×10^{-5} M) was irradiated with 365 nm light at 23 °C for 5 s, and its UV−vis spectrum was measured. The solution was then irradiated with light (λ = ca. 410 nm) at room temperature for 5 s, and its UV−vis spectrum was measured. These operations were repeated 10 times, and the intensities of the band at 265 nm were plotted (Figure 12). As a result, no decrease in the band intensities could be observed even after 10 cycle switching operations, and this indicated that system **1** has good resistance against photofatigue. Thus, we have confirmed that the *stiff*-stilbene core has efficient photochemical *cis*−*trans* isomerization properties.

Anion Binding Properties. Then we started to examine the molecular recognition phenomena of *cis*- and *trans*-(*R*,*R*)-**1**. In recent years, the anion receptors via hydrogen bonds based on NH groups of pyrrole, thiourea, and amide moieties[25] as well as OH groups of alcohol,[26a] phenol,[26b] and silanols[26c] have been reported. We first studied anion recognition in organic solvents by taking advantage of the hydroxyl groups of the BINOL

(25) For examples of NH-based anion receptors, see: Schrader, T.; Hamilton, A. D. *Functional Synthetic Receptors*; Wiley-VCH: New York, 2005; Chapter 4.

(26) (a) Kondo, S.; Suzuki, T.; Yano, Y. *Tetrahedron Lett.* **2002**, *43*, 7059−7061. (b) Kondo, S.; Suzuki, T.; Toyama, T.; Yano, Y. *Bull. Chem. Soc. Jpn.* **2005**, *78*, 1348−1350. (c) Kondo, S.; Harada, T.; Tanaka, R.; Unno, M. *Org. Lett.* **2006**, *20*, 4621−4624.

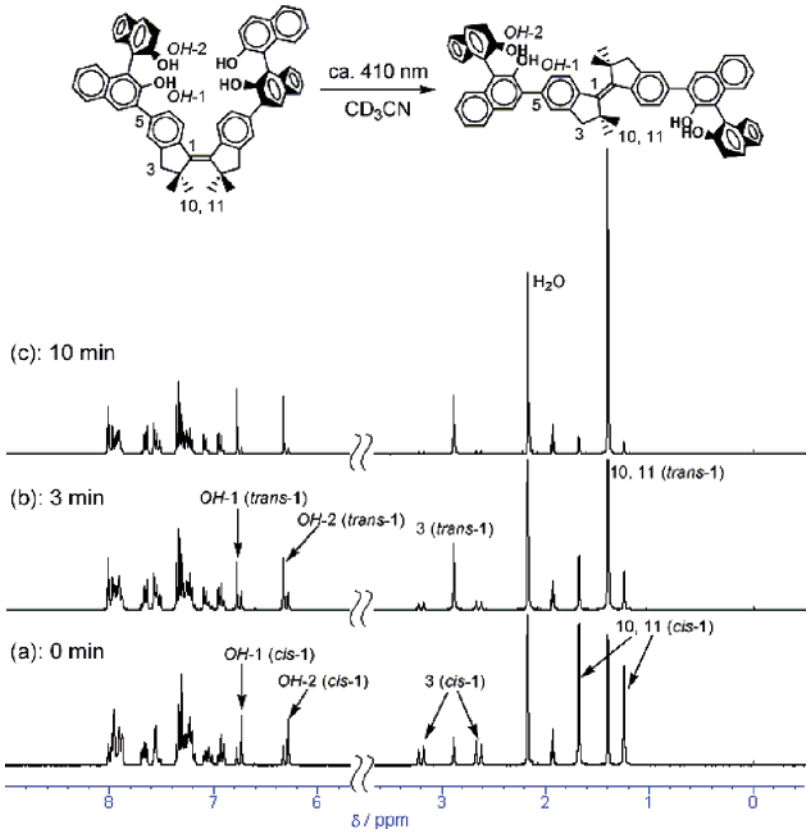

FIGURE 9. ^{1}H NMR spectra of the photoisomerization of *cis*-(*R*,*R*)-**1** to *trans*-(*R*,*R*)-**1** upon irradiation with ca. 410 nm light in CD_3CN: (a) 0 min [*cis*-(*R*,*R*)-**1**/*trans*-(*R*,*R*)-**1** = 75/25], (b) 3 min, (c) 10 min [*trans*-(*R*,*R*)-**1**/*cis*-(*R*,*R*)-**1** = 91/9 (photostationary state)].

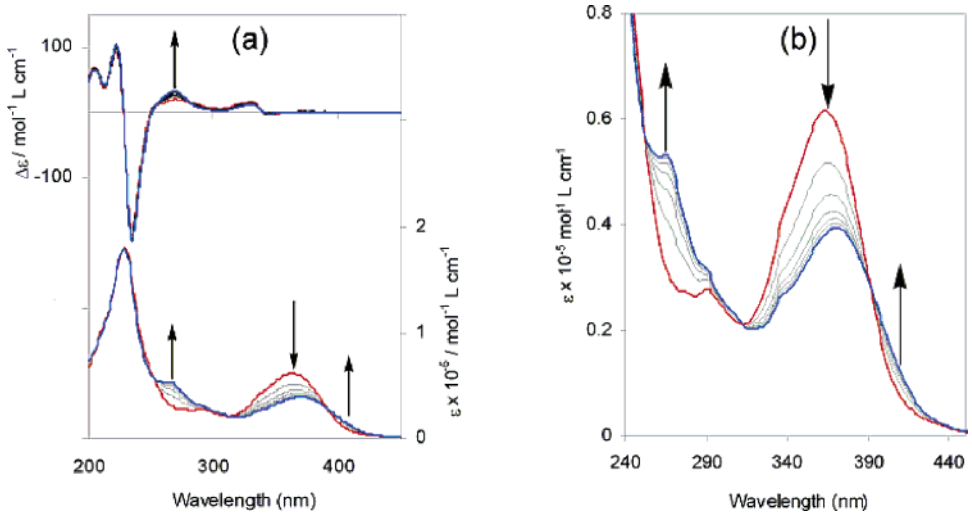

FIGURE 10. Changes in the CD spectra (a) and UV−vis absorption spectra (b) of *trans*-(*R*,*R*)-**1** upon irradiation with 365 ± 5 nm light from a Xe lamp in CH_3CN at 23 °C: 0 min (shown with a red line), 10, 20, 30, 40, and 50 (thin black lines), and 60 min (photostationary state) (blue line).

moieties. The anion recognition properties of *trans*-(*R*,*R*)-**1** with F^-, Cl^-, and $H_2PO_4^-$ in $CDCl_3$ solution were examined by the ^{1}H NMR titration technique (Scheme 3). To a $CDCl_3$ solution (1.0×10^{-3} mol/L) of *trans*-(*R*,*R*)-**1** was added gradually tetrabutylammonium chloride (0 to 2.0×10^{-3} mol/L) at 23 °C (Figure 13). The proton signal of the hydroxyl group (OH-2) of *trans*-(*R*,*R*)-**1** showed a strong downfield shift (up to ca. 1 ppm) with significant broadening upon addition of the tetrabutylammonium chloride. We determined the association constant using the H12 and H17 proton signals because the OH-2 proton signal gradually broadened with an increase of the host/guest ratio. The association constant of the complexation was calculated by a nonlinear curve fitting with the 1/1 model by the ^{1}H NMR titrations because the 1/1 stoichiometry was determined by the ^{1}H NMR measurement. The association constants of *trans*-(*R*,*R*)-**1** were $(1.0 \pm 0.13) \times 10^3$ for F^- ($R = 0.9970$) and $(4.6 \pm 0.72) \times 10^2$ M^{-1} for Cl^- ($R = 0.9993$) in $CDCl_3$ solution. In the case of $H_2PO_4^-$, however, it did not

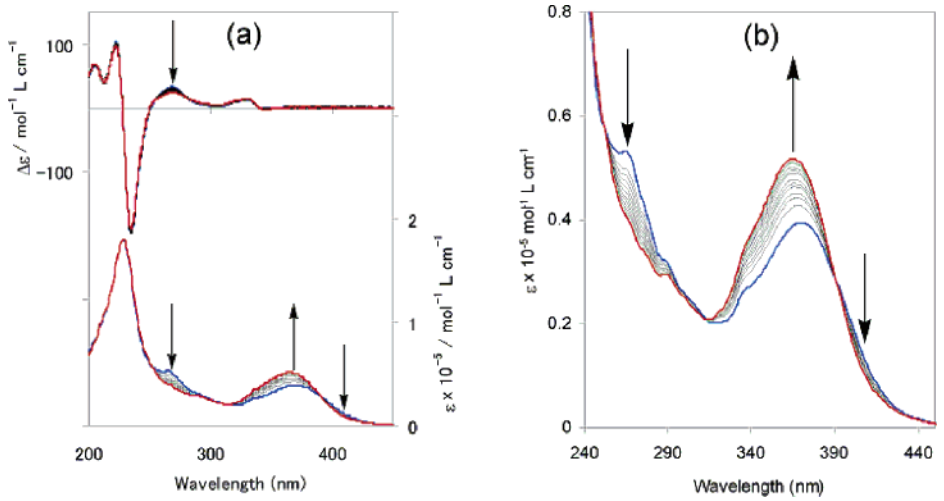

FIGURE 11. Changes in the CD spectra (a) and UV−vis absorption spectra (b) of *cis*-(*R*,*R*)-**1** upon irradiation with 410 ± 5 nm light from a Xe lamp in CH_3CN at 23 °C: 0 (blue line), 10, 20, 30, 40, 50, 60, 70, 80, and 90 (thin black lines), and photostationary state (after 100 min, red line).

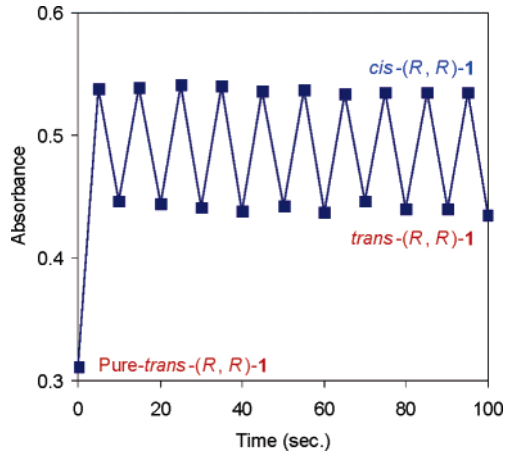

FIGURE 12. Repetitive switching experiments were carried out by monitoring the 265 nm absorption band: irradiation of *trans*-(*R*,*R*)-**1** with 365 nm light and irradiation of *cis*-(*R*,*R*)-**1** with ca. 410 nm light in a CH_3CN solution at 23 °C.

fit the 1/1 and 1/2 model curves, suggesting multistep equilibrium to form the complex.

Similarly, the association constants of *cis*-(*R*,*R*)-**1** with F^-, Cl^-, and $H_2PO_4^-$ were also determined (Scheme 4). The sample of *cis*-(*R*,*R*)-**1** for this study was prepared by the irradiation (365 nm) of the pure *trans*-(*R*,*R*)-**1** in benzene in a Pyrex sample tube for 1 h at 23 °C (Figure 14). The association constants were calculated by a nonlinear curve fitting with the 1/1 model by the data of ^1H NMR titrations using the H12 and H17 signals and determined to be $(1.0 \pm 0.13) \times 10^3$ for F^- ($R = 0.9970$), $(5.9 \pm 0.69) \times 10$ for Cl^- ($R = 0.9993$), and $(9.38 \pm 2.67) \times 10$ M^{-1} for $H_2PO_4^-$ ($R = 0.9948$) in $CDCl_3$ solution. Similar interaction with F^- and Cl^- was observed in *trans*-**1** and *cis*-**1**, but $H_2PO_4^-$ interacted differently: the *cis*-isomer formed the 1/1 complex, whereas multistep equilibrium was expected for the *trans*-isomer. The order of the association constants (F^- > Cl^-) corresponds to the basicity of the anions. Only one BINOL moiety of *trans*-(*R*,*R*)-**1** may interact with the anion because the ^1H NMR data are in good agreement to the 1/1 fitting model. The MO calculations suggested that a Cl^- anion would interact with the hydroxyl groups of the BINOL 2-OH and 2′-OH of *cis*-(*R*,*R*)-**1** (Figure 15), while the four hydroxyl groups may form hydrogen bonds with the oxygen atoms of the guest $H_2PO_4^-$ anion (Figure 16).

Conclusions

New types of functional molecules having a *stiff*-stilbene core as a *cis*−*trans* photochemical isomerization moiety and a BINOL as a chiral recognition moiety have been developed as the first generation of photoswitchable chiral host molecules. *trans*-(*R*,*R*)-**1** was synthesized via Suzuki−Miyaura coupling followed by McMurry coupling as the key reactions from the enantiopure precursors BINOL-indanone **10**. They were characterized by NMR, UV−vis, and CD spectra, specific rotation, and theoretical calculations. *trans*-(*R*,*R*)-**1** showed a relatively intense negative Cotton effect at β-transitions on the naphthyl moiety, and this reflected the counterclockwise chirality in the CD spectrum and positive specific rotation, whereas the CD spectrum of *trans*-(*S*,*S*)-**1** showed the almost complete mirror image. Irradiation of the deoxygenated C_6D_6 solution of pure *trans*-(*R*,*R*)-**1** with 365 nm light led to an 86/14 (*cis*/*trans*)

SCHEME 3. Complex Formation of *trans*-(*R*,*R*)-1 with an Anion

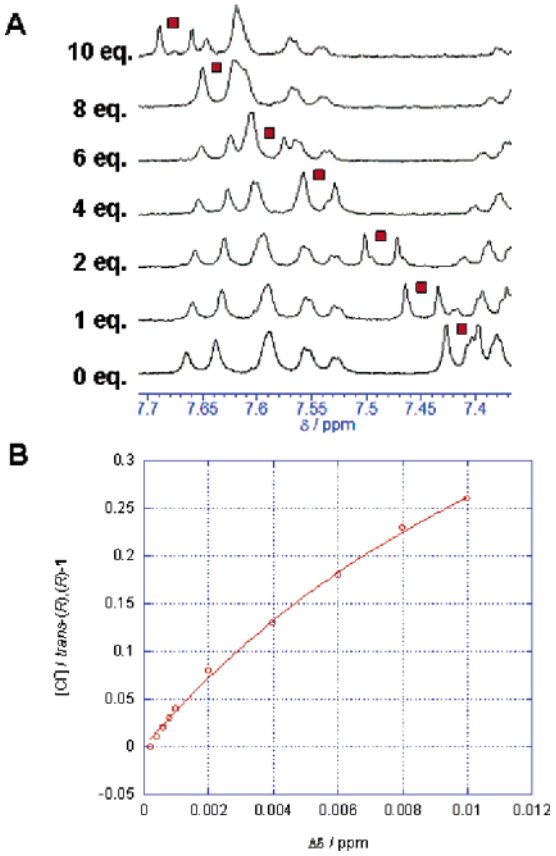

FIGURE 13. (A) ^{1}H NMR titration of *trans*-(*R*,*R*)-**1** with tetrabutylammonium chloride in $CDCl_3$ at 23 °C. The red squares on the spectra correspond to H_{17} of *trans*-(*R*,*R*)-**1**. (B) Nonlinear curve between *trans*-(*R*,*R*)-**1** and tetrabutylammonium chloride in $CDCl_3$ at 23 °C. [*trans*-(*R*,*R*)-**1**] = 1.0×10^{-3} mol/L^{-1}, and [Cl^-] = 0 to 2.0×10^{-3} mol/L.

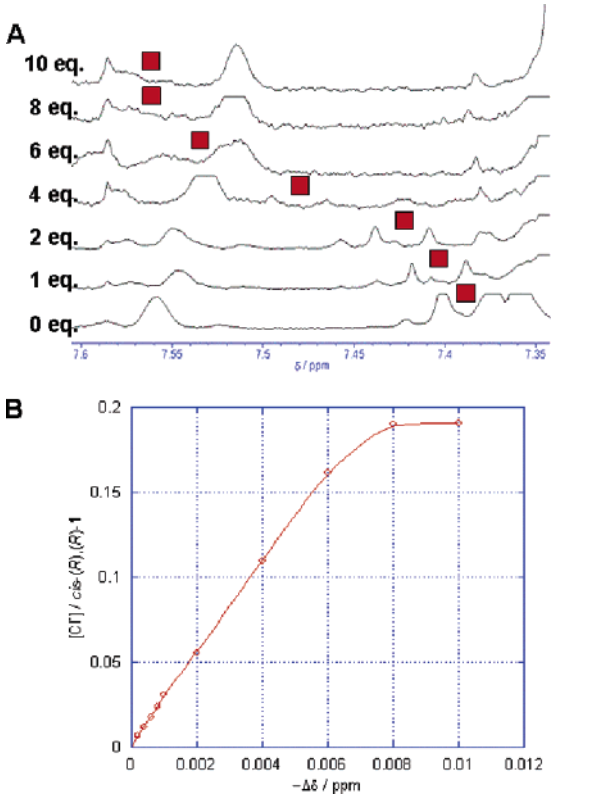

FIGURE 14. (A) ^{1}H NMR titration of *cis*-(*R*,*R*)-**1** with tetrabutylammonium phosphate in $CDCl_3$ at 23 °C. The red squares on the spectra correspond to H_{17} of *cis*-(*R*,*R*)-**1**. (B) Nonlinear curve between *cis*-(*R*,*R*)-**1** and tetrabutylammonium phosphate in $CDCl_3$ at 23 °C. [*cis*-(*R*,*R*)-**1**] = 1.0×10^{-3} mol/L^{-1}, and [$H_2PO_4^-$] = 0 to 2.0×10^{-3} M^{-1}.

mixture at the photostationary state. A mixture of 75/25 (*cis*/*trans*) obtained by irradiation with ca. 410 nm light led to a 23/77 (*cis*/*trans*) mixture at the photostationary state in CH_3CN without decomposition. After 10 repetitions of the *cis*−*trans* interconversions, no decomposition of the *stiff*-stilbene core was observed. The B3LYP/6-31G*-optimized structure predicted that all the hydroxyl groups would be directed toward the inside of the molecule and form the chiral cavity for inclusion in *cis*-(*R*,*R*)-**1**, while the formation of the intramolecular cavity could not be expected for *trans*-(*R*,*R*)-**1**. The structure of *trans*-(*R*,*R*)-**1** was confirmed as the DME adduct via hydrogen bonds between the BINOL OH and ether oxygen by X-ray structural study. The guest binding properties of the BINOL moieties of *trans*-(*R*,*R*)-**1** and *cis*-(*R*,*R*)-**1** with F^-, Cl^-, and $H_2PO_4^-$ were examined, and the *trans*- and *cis*-isomers showed similar interaction with F^- and Cl^- (host/guest = 1/1), but $H_2PO_4^-$ interacted in a different way: the *cis*-isomer formed a 1/1 complex, but multistep equilibrium was expected for the *trans*-isomer. A detailed study on the structure of these complexes and examination of other guest molecules are in progress. The design and synthesis of the second-generation photoswitchable host molecules with a *stiff*-stilbene core, which should satisfy the inclusion in the *cis*-form and release the guest in the *trans*-form upon irradiation, should be the next problem to be solved. These results will be reported elsewhere in due time.

Experimental Section

Methyl 3-(3-Bromophenyl)-2,2-dimethylpropionate (4). A mixture of 3-bromotoluene (**2**) (10.0 g, 58.5 mmol) and benzene (50 mL) was heated at ca. 70 °C under an Ar atomosphere. NBS (10.4 g, 58.5 mmol) and AIBN (ca. 50 mg) were added to this solution, and the mixture was refluxed for 10 h. After the resulting yellow solution was cooled to room temperature, the precipitate

SCHEME 4. Complex Formation of *cis*-(*R*,*R*)-1 with an Anion

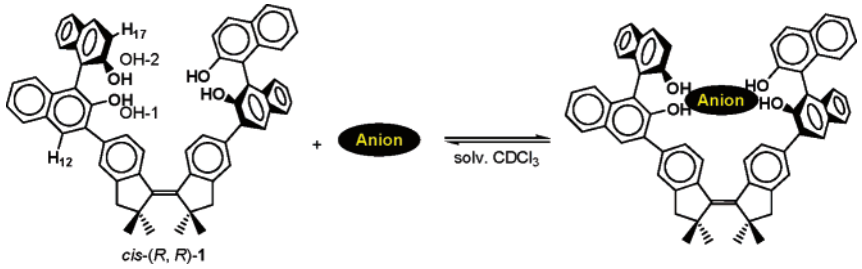

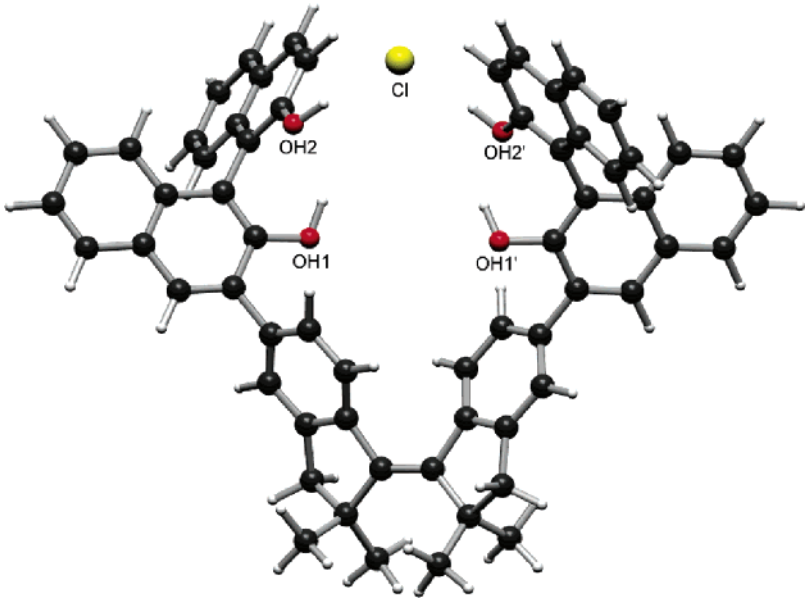

FIGURE 15. Optimized structure of the complex between *cis*-(*R*,*R*)-**1** and the Cl anion at the HF/6-31G* level of theory. Selected hydrogen bond lengths (Å): OH2−Cl, 2.249; OH2′−Cl, 2.208.

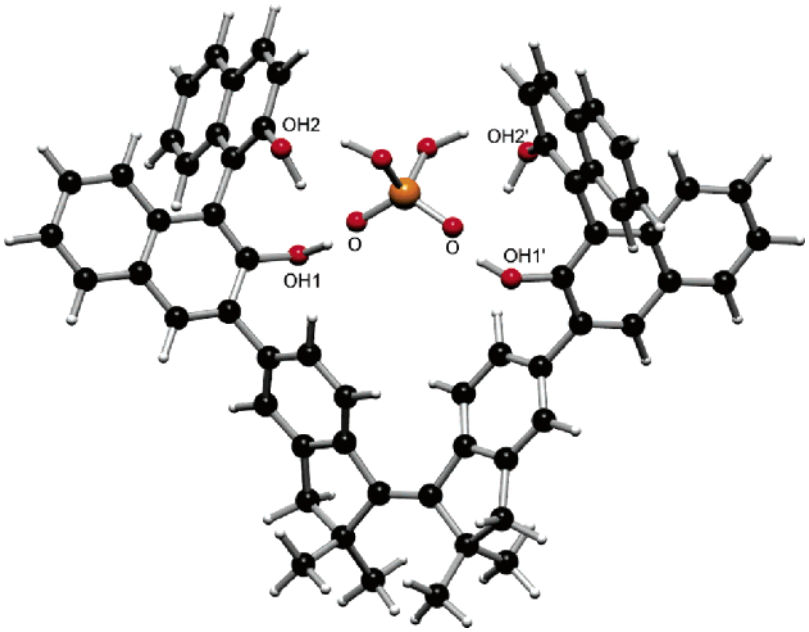

FIGURE 16. Optimized structure of the complex between *cis*-(*R*,*R*)-**1** and the H_2PO_4 anion at the HF/6-31G* level of theory. Selected hydrogen bond lengths (Å): OH1−O, 1.584; OH2−O, 1.668; OH1′−O, 1.584; OH2−O, 1.667.

was removed by filtration, and the filtrate was concentrated under reduced pressure to afford the desired 1-bromo-3-(bromomethyl)-benzene (**3**)[13] as yellow crystals, which were used in the next reaction without further purification: ^{1}H NMR (300 MHz, $CDCl_3$) δ 4.38 (2H, s, benzyl H_2), 7.17−7.26 (2H, m, Ar *H*), 7.39 (1H, d, J = 6.24 Hz, Ar *H*), 7.50 (1H, d, J = 1.47 Hz, Ar *H*); ^{13}C NMR (75 MHz, $CDCl_3$) δ 32.0 (benzyl), 122.5 (Ar), 127.5 (Ar), 128.2 (Ar), 130.2 (Ar), 131.4 (Ar), 131.9 (Ar).

To LDA in THF[2n] was added methyl 2-methylpropionate (3.06 g, 29.3 mmol) in one portion for 30 min at −78 °C. To the mixture was added dropwise 3-bromobenzyl bromide (**3**) over a period of 1 h at −78 °C. Then, the mixture was allowed to warm to room temperature and stirred at room temperature for an additional 12 h. The reaction mixture was quenched by the addition of water and extracted with diethyl ether, the combined ether extracts were dried over $MgSO_4$ and filtered, and the filtrate was concentrated under reduced pressure. The crude product was purified by column chromatography on silica gel with hexane/CH_2Cl_2 (7/3) as an eluent to give **4 (**10.2 g, 37.4 mmol, 64% in two steps) as a slightly yellow viscous oil: ^{1}H NMR (300 MHz, $CDCl_3$) δ 1.19 (6H, s, −CH_3), 2.83 (2H, s, benzyl H_2), 3.68 (3H, s, −OCH_3), 7.14 (1H, t, J = 7.5 Hz, Ar *H*), 7.27 (1H, s, Ar *H*), 7.36 (1H, d, J = 7.8 Hz, Ar *H*); ^{13}C NMR (75 MHz, $CDCl_3$) δ 24.9 (−Me), 43.6 (benzyl), 45.9 (quaternary C), 51.7 (−OMe), 122.1 (Ar), 128.7 (Ar), 129.5 (Ar), 129.6 (Ar), 133.0 (Ar), 140.2 (Ar), 177.5 (carbonyl); IR (neat on NaCl plates) 1473.4 [ν(C═O)] cm^{-1}; HRMS (FAB) *m*/*z* calcd for $C_{12}H_{15}{}^{79}BrO_2$ 271.0334 [M^+], found 271.0332. Anal. Calcd for

$C_{12}H_{15}BrO_2 \cdot 0.25CH_2Cl_2$: C, 50.10; H, 5.23. Found: C, 50.32; H, 5.34.

3-(3-Bromophenyl)-2,2-dimethylpropionic Acid (5). To a mixture of the ester **4** (9.46 g, 36.8 mmol), H_2O (40 mL), and MeOH (10 mL) was added KOH (20.8 g, 368 mmol), and the mixture was refluxed overnight. The slightly yellow solution was cooled and acidified with 6 N HCl. The white precipitate was extracted with diethyl ether, and the combined ether extracts were washed with water several times, dried over $MgSO_4$, and filtered. The filterate was concentrated under reduced pressure, and the concentrate was recrystallized from CH_2Cl_2/hexane to give the carboxylic acid **5** as colorless crystals (9.00 g, 35.0 mmol, 95%): mp 53−54 °C; ^{1}H NMR (300 MHz, $CDCl_3$) δ 1.21 (6H, s, $-CH_3$), 2.86 (2H, s, benzyl H_2), 7.08−7.11 (1H, m, Ar *H*), 7.14 (1H, t, J = 7.5 Hz, Ar *H*), 7.32 (1H, s, Ar *H*), 7.35−7.38 (1H, m, Ar *H*); ^{13}C NMR (75 MHz, $CDCl_3$) δ 24.6 (−Me), 24.7 (−Me), 43.4 (benzyl), 45.3 (quaternary C), 122.1 (Ar), 128.8 (Ar), 129.6 (Ar), 133.2 (Ar), 139.8 (Ar), 183.6 (carbonyl); IR (KBr) 1697.1 [ν(C=O)] cm^{-1}; HRMS (FAB) *m*/*z* calcd for $C_{11}H_{13}{}^{79}BrO_2$ 256.0099 [M$^+$], found 256.0093. Anal. Calcd for $C_{11}H_{13}BrO_2$: C, 51.37; H, 5.09. Found: C, 51.38; H, 5.10.

5-Bromo-2,2-dimethyl-1-indanone (6). Thionyl chloride (6.4 mL, 83.8 mmol) was added dropwise to the carboxylic acid **5** (6.73 g, 26.2 mmol), and the mixture was heated at 50 °C for 2 h. The excess thionyl chloride was removed by evaporation under reduced pressure, and the resultant yellow oil was used in the next reaction without further purification.

To a CH_2Cl_2 solution (100 mL) of the acid chloride was slowly added $AlCl_3$ (7.00 g, 52.4 mmol), and then the mixture was stirred at room temperature for 1 h. The reaction mixture was quenched with satd aq NH_4Cl solution and was extracted with CH_2Cl_2 several times. The combined CH_2Cl_2 extracts were washed with H_2O, dried over $MgSO_4$, and filtered, and the filtrate was evaporated under reduced pressure to give the crude product, which was purified by column chromatography on silica gel with CH_2Cl_2/hexane (3/7) as an eluent to give the indanone **6** (5.10 g, 21.3 mmol, 82% in two steps) as a viscous colorless oil: ^{1}H NMR (300 MHz, $CDCl_3$) δ 1.23 (6H, s, $-CH_3$), 2.98 (2H, s, benzyl H_2), 7.49 (1H, d, J = 8.1 Hz, Ar *H*), 7.59−7.61 (2H, m, Ar *H*) [lit.[12] ^{1}H NMR ($CDCl_3$) δ 1.24 (s, 6H), 2.99 (s, 2H), 7.50−7.53 (m, 1H), 7.61−7.63 (m, 2H)]; ^{13}C NMR (75 MHz, $CDCl_3$) δ 25.2 (Me), 42.5 (benzyl), 45.7 (quaternary C), 125.7 (Ar), 129.9 (Ar), 130.1 (Ar), 131.0 (Ar), 134.0 (Ar), 153.8 (Ar), 210.0 (carbonyl); IR (neat on NaCl plates) 1708.6 [ν(C=O)] cm^{-1}.

(*R*)- and (*S*)-1,1′-Binaphthyl 2,2′-Bis(methoxymethyl) Diether [(*R*)-8 and (*S*)-8]. These compounds were prepared according to the literature procedures.[15b] Data for (*R*)-**8** (99%): colorless crystals (from benzene); mp 91−92 °C (lit.[15b] mp 89−92 °C). Data for (*S*)-**8** (98%): colorless crystals (from benzene); mp 90−92 °C (lit.[15c] mp 95−97 °C).

2,2′-Bis(methoxymethoxy)-3-(2,2-dimethylindanon-5-yl)-(*R*)-1,1′-binaphthyl [(*R*)-10]. A dry THF solution (40 mL) of (*R*)-**8** (2.00 g, 5.34 mmol) was cooled to −78 °C under an Ar atmosphere. To this mixture was added slowly a 1.54 M hexane solution of *n*-BuLi (4.5 mL, 6.94 mmol) from a syringe. After the mixture was stirred for 4 h at −78 °C, $B(OMe)_3$ (0.6 mL, 5.34 mmol) was added in one portion to this solution. The reaction mixture was allowed to warm to room temperature and stirred at room temperature for 12 h. The reaction mixture was quenched with H_2O and extracted with diethyl ether. The combined diethyl ether extracts were washed with water, dried over $MgSO_4$, and filtered, and the filtrate was evaporated under reduced pressure to give (*R*)-**9** as a colorless oil, which was used for the next reaction without further purification.

To a toluene solution (30 mL) of the borate (*R*)-**9** were added **6** (1.41 g, 5.87 mmol) and saturated Na_2CO_3 solution (20 mL), which was deoxygened with Ar bubbling. After 30 min, $Pd(PPh_3)_4$ (309 mg, 267 μmol) was added, and the mixture was refluxed for 12 h. The cooled reaction mixture was washed with brine, dried over $MgSO_4$, and filtered. The filtrate was concentrated under reduced pressure, and the concentrate was purified by column chromatography on silica gel with CH_2Cl_2 as an eluent to give (*R*)-**10** [1.89 g, 3.56 mmol, 67% (from (*R*)-**8**)] as colorless crystals (benzene): mp 95−96 °C; $[\alpha]^{24}_D$ +168.3 (c = 1.00, CH_3CN); ^{1}H NMR (300 MHz, $CDCl_3$) δ 1.28 (6H, s, $-CH_3$), 3.07 (2H, s, benzyl H_2), 3.20 (6H, s, $-OCH_3$), 4.31, 4.39 (2H, d, AB, J_{AB} = 6.0 Hz, OCH_2O), 5.07, 5.19 (2H, d, AB, J_{AB} = 6.9 Hz, OCH_2O), 7.22−7.46 (6H, m, Ar *H*), 7.61 (1H, d, J = 9.0 Hz, Ar *H*), 7.74−7.98 (7H, m, Ar *H*); ^{13}C NMR (75 MHz, $CDCl_3$) δ 25.4 [−Me (indanone)], 42.9 (benzyl), 45.8 (quaternary C), 55.9 (−OMe), 56.0 (−OMe), 95.1 (OCH_2O), 99.0 (OCH_2O), 116.7 (Ar), 120.9 (Ar), 124.2 (Ar), 125.4 (Ar), 125.6 (Ar), 125.9 (Ar), 126.6 (Ar), 127.7 (Ar), 127.9 (Ar), 128.1 (Ar), 129.4 (Ar), 129.7 (Ar), 129.9 (Ar), 130.5 (Ar), 130.8 (Ar), 133.7 (Ar), 133.9 (Ar), 134.0 (Ar), 134.8 (Ar), 146.1 (Ar), 150.9 (Ar), 152.3 (Ar), 152.9 (Ar), 211.1 (carbonyl); IR (KBr disk) 1712.5 [ν(C=O)] cm^{-1}; CD (CH_3CN) λ ($\Delta\epsilon$) 222.0 (31), 234.5 (−90), 272.0 (43), 330.0 (−5) nm; UV (CH_3CN) λ (ϵ) 228.6 (96 000), 275.2 (31 000), 292.8 (27 000, sh), 331.8 (6000, sh) nm; HRMS (FAB) *m*/*z* calcd for $C_{35}H_{32}O_5$ 532.2250 [M$^+$], found 532.2252. Anal. Calcd for $C_{35}H_{32}O_5 \cdot 0.5H_2O$: C, 78.61; H, 6.14. Found: C, 78.57; H, 6.08.

2,2′-Bis(methoxymethoxy)-3-(2,2-dimethylindanon-5-yl)-(*S*)-1,1′-binaphthyl [(*S*)-10]. (*S*)-**10** was also synthesized by procedures similar to those described for (*R*)-**10**. Starting from (*S*)-**8** (3.00 g, 8.00 mmol), (*S*)-**10** was obtained as colorless crystals in 57% yield (2.44 g, 4.58 mmol): mp 96−97 °C; $[\alpha]^{24}_D$ −166.9 (c = 1.01, CH_3CN); ^{1}H NMR (300 MHz, $CDCl_3$) δ 1.28 (6H, s, $-CH_3$), 3.07 (2H, s, benzyl H_2), 3.20 (6H, s, $-OCH_3$), 4.31, 4.39 (2H, d, AB, J_{AB} = 6.0 Hz, OCH_2O), 5.07, 5.19 (2H, d, AB, J_{AB} = 6.9 Hz, OCH_2O), 7.22−7.46 (6H, m, Ar *H*), 7.61 (1H, d, J = 9.0 Hz, Ar *H*), 7.74−7.98 (7H, m, Ar *H*); ^{13}C NMR (75 MHz, $CDCl_3$) δ 25.3 [−Me (indanone)], 42.9 (quaternary C), 45.8 (benzyl), 55.9 (−OMe), 56.0 (−OMe), 95.1 (OCH_2O), 99.0 (OCH_2O), 116.7 (Ar), 120.8 (Ar), 124.2 (Ar), 125.4 (Ar), 125.6 (Ar), 125.9 (Ar), 126.6 (Ar), 127.7 (Ar), 127.9 (Ar), 128.1 (Ar), 129.4 (Ar), 129.7 (Ar), 129.8 (Ar), 130.4 (Ar), 130.8 (Ar), 133.7 (Ar), 133.9 (Ar), 134.0 (Ar), 134.8 (Ar), 146.0 (Ar), 150.8 (Ar), 152.2 (Ar), 152.8 (Ar), 211.1 (carbonyl); IR (KBr) 1712.5 [ν(C=O)] cm^{-1}; CD (CH_3CN) λ ($\Delta\epsilon$) 222.0 (−25), 234.5 (87), 272.0 (−34), 330.0 (3) nm; UV (CH_3CN) λ (ϵ) 228.6 (96 000), 275.2 (31 000), 292.8 (27 000, sh), 331.8 (6000, sh) nm; HRMS (FAB) *m*/*z* calcd for $C_{35}H_{32}O_5$ 532.2250 [M$^+$], found 532.2171. Anal. Calcd for $C_{35}H_{32}O_5 \cdot 0.4H_2O$: C, 78.87; H, 6.12. Found: C, 78.93; H, 6.13.

***trans*-2,2,2′,2′-Tetramethyl-5,5′-Bis[(*R*)-2,2′-binaphthol-3,3′-yl]-1,1′-indanylindane [*trans*-(*R*,*R*)-1].** To a suspension of $TiCl_4$ (1.3 mL, 9.33 mmol) in dry THF (10 mL) was slowly added Zn powder (1.23 g, 18.7 mmol) under an Ar atmosphere. The resultant deep red slurry was heated at reflux for 1 h. The THF solution (5 mL) of (*R*)-**10** (1.65 g, 3.11 mmol) was added to the mixture in one portion, and the mixture was refluxed for 12 h. The reaction mixture was quenched with satd aq NH_4Cl solution and was extracted with diethyl ether. The combined ether extracts were dried over $MgSO_4$, and the filtrate was concentrated under reduced pressure. The crude product was used for the next reaction without further purification.

To a mixture of the crude product, CH_2Cl_2 (10 mL), and methanol (5 mL) was added 6 N HCl (3 drops), and the mixture was refluxed for 12 h. The mixture was poured into water and was extracted with CH_2Cl_2. The combined CH_2Cl_2 solution was dried over $MgSO_4$ and filtered, and the filtrate was concentrated under reduced pressure to give the crude product (*cis*/*trans* = ca. 1/5), which was purified by column chromatography on silica gel with CH_2Cl_2/hexane (7/3) as an eluent, followed by precipitation from CH_2Cl_2/hexane to give pure *trans*-(*R*,*R*)-**1** (381.7 mg, 446 μmol, 29% in two steps) as a slightly yellow powder: mp 225−226 °C dec; $[\alpha]^{24}_D$ +205.4 (c = 0.55, CH_3CN); ^{1}H NMR (600 MHz, CD_3CN) δ 1.41 (12H, s, $-CH_3$), 2.89 (4H, s, benzyl H_2), 6.31 (2H, br s, $-OH$), 6.71 (2H, br s, $-OH$), 6.94 (2H, d, J = 8.4 Hz, Ar *H*), 7.09 (2H, d, J = 8.4

Hz, Ar *H*), 7.25 (2H, ddd, J = 1.2, 6.6, and 7.8 Hz, Ar *H*), 7.28 (2H, ddd, J = 1.2, 6.6, and 7.8 Hz, Ar *H*), 7.34 (4H, m, Ar *H*), 7.35 (2H, d, J = 8.4 Hz, Ar *H*), 7.54 (2H, dd, J = 1.8 and 8.4 Hz, Ar *H*), 7.58 (2H, s, Ar *H*), 7.66 (2H, d, J = 8.4 Hz, Ar *H*), 7.93 (2H, d, J = 8.4 Hz, Ar *H*), 7.95 (2H, d, J = 8.4 Hz, Ar *H*), 8.00 (2H, d, J = 9.0 Hz, Ar *H*), 8.03 (2H, s, Ar *H*); ^{13}C NMR (150 MHz, CD_3CN) δ 27.90 (−Me), 27.92 (−Me) 51.5 (benzyl), 52.6 (quaternary C), 113.9 (Ar), 115.2 (Ar), 119.5 (Ar), 124.4 (Ar), 124.6 (Ar), 125.0 (Ar), 125.1 (Ar), 126.4 (Ar), 127.55 (Ar), 127.58 (Ar), 127.8 (Ar), 128.7 (Ar), 129.19 (Ar), 129.25 (Ar), 130.3 (Ar), 130.4 (Ar), 131.2 (Ar), 131.6 (Ar), 132.2 (Ar), 134.5 (Ar), 135.2 (Ar), 138.5 (Ar), 142.8 (Ar), 146.3 (Ar), 147.1 (C═C), 151.8 (Ar) 154.7 (Ar); IR (KBr) 3512.7 [ν(O−H)] cm^{-1}; CD (CH_3CN) λ ($\Delta\epsilon$) 221.5 (88), 234.5 (−190), 267.5 (20), 328.5 (18) nm; UV (CH_3CN) λ (ϵ) 228 (2 000 000), 290 (29 200), 335 (40 300, sh), 363 (61 500) nm; MS (FAB, HR) *m*/*z* calcd for $C_{62}H_{48}O_4$ 856.3553 [M$^+$], found 856.3558. Anal. Calcd for $C_{62}H_{48}O_5 \cdot 0.8H_2O$: C, 85.45; H, 5.74. Found: C, 85.41; H, 5.63.

***trans*-2,2,2′,2′-Tetramethyl-5,5′-Bis[(*S*)-2,2′-binaphthol-3,3′-yl]-1,1′-indanylindane [*trans*-(*S*,*S*)-1].** This compound was synthesized by procedures similar to those described for *trans*-(*R*,*R*)-**1**. Starting from (*S*)-**10** (1.65 g, 3.11 mmol), *trans*-(*S*,*S*)-**1** was obtained as a slightly yellow color powder in 21% yield (228 mg, 266 mmol): mp 225−227 °C dec; $[\alpha]^{24}_D$ −205.6 (c = 1.00, CH_3CN); ^{1}H NMR (300 MHz, $CDCl_3$) δ 1.42 (12H, s, −CH_3), 2.88 (4H, br s, benzyl H_2), 5.13 (2H, s, −O*H*), 5.42 (2H, s, −O*H*), 7.16 (2H, br d, J = 8.1 Hz, Ar *H*), 7.23−7.42 (12H, m, Ar *H*), 7.55 (2H, br t, J = 8.0 Hz, Ar *H*), 7.59 (2H, br s, Ar *H*), 7.65 (2H, d, J = 8.0 Hz, Ar *H*), 7.92 (4H, br t, J = 9.0 Hz, Ar *H*), 7.99 (2H, d, J = 9.0 Hz, Ar *H*), 8.10 (2H, s, Ar *H*); ^{13}C NMR (75 MHz, $CDCl_3$) δ 27.7 (−Me), 27.8 (−Me), 50.8 (benzyl), 52.0 (quaternary C), 111.7 (Ar), 111.8 (Ar), 123.9 (Ar), 124.2 (Ar), 124.36 (Ar), 124.37 (Ar), 125.3 (Ar), 126.3 (Ar), 127.3 (Ar), 127.4 (Ar), 128.0 (Ar), 128.39 (Ar), 128.43 (Ar), 129.4 (Ar), 129.5 (Ar), 130.7 (Ar), 131.2 (Ar), 132.9 (Ar), 133.5 (Ar), 136.0 (Ar), 142.4 (Ar), 145.7 (Ar), 146.2 (C═C), 150.3 (Ar), 152.6 (Ar); IR (KBr) 3471.2 [ν(O−H)] cm^{-1}; CD (CH_3CN) λ ($\Delta\epsilon$) 221.5 (90), 234.5 (−180), 267.5 (23), 328.5 (15) nm; UV (CH_3CN) λ (ϵ) 228 (2 000 000), 290 (29 200), 335 (40 300, sh), 363 (61 500) nm; HRMS (FAB) *m*/*z* calcd for $C_{62}H_{48}O_4$ 857.0607 [M$^+$], found 857.0644. Anal. Calcd for $C_{35}H_{32}O_5 \cdot 0.5H_2O$: C, 85.98; H, 5.70. Found: C, 86.33, H, 6.09.

***cis*-2,2,2′,2′-Tetramethyl-5,5′-Bis[(*R*)-2,2′-binaphthol-3,3′-yl]-1,1′-indanylindane [*cis*-(*R*,*R*)-1].** *cis*-(*R*,*R*)-**1** was highly unstable to silica gel and the room light. Formation of *cis*-(*R*,*R*)-**1** was detected by ^{1}H NMR, UV−vis, and CD spectra as a mixture of *cis*-(*R*,*R*)-**1**/*trans*-(*R*,*R*)-**1** in 86/14 and 75/25 ratios in benzene and CH_3CN solution, respectively. The NOE data of *cis*-(*R*,*R*)-**1** are shown in Figures S19 and S20.

Binding Constant Determination. Stock solutions of **1** (1.0×10^{-3} mol/L^{-1}), host/guest = 1/10 and host/guest = 1/1, in $CDCl_3$ were prepared, and solutions of host/guest = 1/0.2 to 1/10 were prepared using the stock solutions. The ^{1}H NMR spectra were measured and recorded, repeatedly. The association constants were calculated from the chemical shifts of naphthyl H12 and H17 by the nonlinear least-squares fitting program.

Photoisomerization Experiments. As a light source of the isomerization from *trans*-(*R*,*R*)-**1** to *cis*-(*R*,*R*)-**1**, we used black light lamps (10 W × 7, λ = 365 nm). In the reverse isomerization reaction (*cis* to *trans*), we used a Xe lamp in a fluorescence spectrophotometer. These reactions were monitored by UV−vis and CD spectra as well as the ^{1}H NMR spectrum. When we monitored the *cis* to *trans* isomerization by the ^{1}H NMR spectrum, we used an ultra-high-pressure Hg lamp (500 W) with cutoff filters (λ = 300−500 nm and λ = 380−750 nm). The continuous switching experiments were carried out by using a photoreactor which was made up of black light lamps and an ultra-high-pressure Hg lamp (ca. 410 nm). For UV−vis and CD detection, the reactants were dissolved in CH_3CN (10^{-5} M), and then deoxygened with Ar bubbling for 5 min in a quartz cell. The solution was irradiated with 365 ± 5 nm light using a Xe lamp every 10 min at 23 °C, and the process was monitored by UV−vis and CD spectra. The irradiation was continued to reach the photostationary state, and then the solution was irradiated with the 410 ± 5 nm light of a Xe lamp every 10 min at 23 °C. For ^{1}H NMR spectral monitoring, the reactants were dissolved in CD_3CN (as 5×10^{-3} M), and then the mixture was deoxygenated with Ar bubbling for 5 min in an NMR tube. The *trans* to *cis* isomerization process was carried out by the use of 365 nm light at 23 °C and monitored by ^{1}H NMR spectra after 3, 10, 20, 30, and 60 min. The *cis* to *trans* process was performed by irradiation via an ultra-high-pressure Hg lamp (λ = ca. 410 nm) of the solution at 23 °C, and ^{1}H NMR spectra were measured after 3 and 10 min of irradiation (photostationary state). The repeated switching experiments were carried out by irradiation of a solution of the enantiopure *trans*-(*R*,*R*)-**1** (1×10^{-5} M) with 365 nm light for 5 s at 23 °C. In the reverse reaction, the *cis*-rich solution was irradiated with light (λ = ca. 410 nm) at room temperature for 5 s, and its UV−vis spectrum was measured.

Theoretical Methods. All calculations were performed using the Gaussian 03[27] suite of programs. Geometry optimizations, frequency calculations, and single-point energy calculations for *trans*-(*R*,*R*)-**1** and the *cis*-(*R*,*R*)-**1** were performed by using Becke's three-parameter hybrid functional (B3)[28] with the correlation functional of Lee, Yang, and Parr (LYP)[29,30] and the Pople style basis set 6-31G*. For the chloro and phosphate anions on *cis*-(*R*,*R*)-**1**, restricted calculations were performed because all relevant species were closed-shell molecules.

Acknowledgment. We greatly acknowledge financial support by a Theme Project of Molecular Architecture of Organic Compounds for Functional Designs (Professor Tahsin J. Chow), Institute of Chemistry, Academia Sinica, Taiwan, ROC. We are also grateful for partial financial support by a Grant-in-Aid for Scientific Research (B) (No. 18350025) from the Ministry of Education, Culture, Sports, Science and Technology, Japan. T.S. also acknowledges partial financial support from the Rikougaku Foundation (Tokyo Institute of Technology TLO). We thank Professor Dr. Junji Inanaga and Dr. Hiroshi Furuno (Kyushu University) for measurement of the CD spectra and specific rotation, Professor Dr. Masaaki Mishima (Kyushu University) for theoretical calculations, Professor Dr. Shuntaro Mataka and Dr. Tsutomu Ishi-i (Kyushu University) for measurement of the IR spectra, and Associate Professor Dr. Minoru Yamaji (Gunma University) for detection of the photochemical switching process.

Supporting Information Available: ^{1}H and ^{13}C NMR spectra of **4**, **5**, **10**, and *trans*-(*R*,*R*)-**1**, ^{1}H−^{1}H COSY, HMBC, HMQC, and NOE spectra of *trans*-(*R*,*R*)-**1**, NOE and ^{13}C NMR spectra of the *cis*-(*R*,*R*)-**1**/*trans*-(*R*,*R*)-**1** mixture (75/25), X-ray crystallographic

(27) Frisch, M. J.; Trucks, G. W.; Schlegel, H. B.; Scuseria, G. E.; Robb, M. A.; Cheeseman, J. R.; Montgomery, J. A., Jr.; Vreven, T.; Kudin, K. N.; Burant, J. C.; Millam, J. M.; Iyengar, S. S.; Tomasi, J.; Barone, V.; Mennucci, B.; Cossi, M.; Scalmani, G.; Rega, N.; Petersson, G. A.; Nakatsuji, H.; Hada, M.; Ehara, M.; Toyota, K.; Fukuda, R.; Hasegawa, J.; Ishida, M.; Nakajima. T.; Honda, Y.; Kitao, O.; Nakai, H.; Klene, M.; Li, X.; knox, J. E.; Hratchian, H. P.; Cross, J. B.; Bakken, V.; Adamo, C.; Jaramillo, J.; Gomperts, R.; Stratmann, R. E.; Yazyev, O.; Austin, A. J.; Cammi, R.; Pomelli, C.; Ochterski, J. W.; Ayala, P. Y.; Morokuma, K.; Voth, G. A.; Salvador, P.; Dannenberg, J. J.; Zakrzewski, V. G.; Dapprich, S.; Daniels, A. D.; Strain, M. C.; Farkas, O.; Malick, D. K.; Rabuck, A. D.; Raghavachari, K.; Foresman, J. B.; Ortiz, J. V.; Cui, Q.; Baboul, A. G.; Clifford, S.; Cioslowski, J.; Stefanov, B. B.; Liu, G.; Liashenko, A.; Piskorz, P.; komaromi, I.; Martin, R. L.; Fox, D. J.; Keith, T.; Al-Lahm, M. A.; Peng, C. Y.; Nanayakkara, A.; Challacombe, M.; Gill, P. M. W.; Johnson, B.; Chen, W.; Wong, M. W.; Gonzales, C.; Pople, J. A. *Gaussian 03*, revision C.02; Gaussian, Inc.: Wallingford, CT, 2004.

(28) Becke, A. D. *J. Chem. Phys.* **1993**, 5648−5652.

(29) Lee, C.; Yang, W.; Parr, R. G. *Phys. Rev. B* **1988**, *37*, 785−789.

(30) Miehlich, B.; Savin, A.; Stoll, H.; Preuss, H. *Chem. Phys. Lett.* **1989**, *157*, 200−206.

structure analysis, ^{1}H NMR titration of *trans*-(*R*,*R*)-**1** with tetrabutylammonium fluoride, ^{1}H NMR titration of *cis*-(*R*,*R*)-**1** with tetrabutylammonium chloride and fluoride, comparison of the rate of *trans* to *cis* and *cis* to *trans* photoisomerization between **1** and azobenzene in benzene, frontier orbitals and coordinates of *trans*-(*R*,*R*)-**1** and *cis*-(*R*,*R*)-**1** at the B3LYP/6-31G* level, coordinates of *cis*-(*R*,*R*)-**1** and Cl^- and $H_2PO_4^-$ complexes at the HF/6-31G* level, and structural data for the X-ray analysis (positional and thermal parameters and bond distances and angles in CIF format) of (*R*)-**10** (CCDC 296829) and *trans*-(*R*,*R*)-**1** (CCDC 624693). This material is available free of charge via the Internet at http://pubs.acs.org.

JO061127V